

Pricing barrier and Bermudan style options under time-changed Lévy processes: fast Hilbert transform approach

Pingping Zeng and Yue Kuen Kwok¹

Department of Mathematics,
Hong Kong University of Science and Technology,
Hong Kong

January, 2014

Abstract

We construct efficient and accurate numerical algorithms for pricing discretely monitored barrier and Bermudan style options under time-changed Lévy processes by applying the fast Hilbert transform method to the log-asset return dimension and quadrature rule to the dimension of log-activity rate of stochastic time change. Some popular stochastic volatility models, like the Heston model, can be nested in the class of time-changed Lévy processes. The computational advantages of the fast Hilbert transform approach over the usual fast Fourier transform method, like exponential decay of errors in terms of the step size in the transform and avoidance of recovering option prices at the monitoring time instants, can be extended to pricing barrier and Bermudan style options under time-changed Lévy processes. We manage to compute the fair value of a dividend-ruin model with both embedded reflecting (dividend) barrier and absorbing (ruined) barrier. We also consider pricing of Bermudan options in conjunction with the determination of the associated critical asset prices. Our numerical tests demonstrate high level of accuracy, efficiency and reliability of the fast Hilbert transform approach when compared to other numerical schemes in the literature.

Keywords: fast Hilbert transform, time-changed Lévy processes, barrier options, dividend-ruin model, Bermudan options

1 Introduction

A discrete path dependent option is a financial derivative whose payoff is dependent on the path realization of the underlying asset price process monitored at discrete time instants throughout the life of the derivative. In the past decades, effective analytical tools have been developed to price various types of continuously monitored path dependent options under different underlying asset price processes. However, most path dependent options traded in the financial markets involve discrete monitoring of the underlying asset price processes. It is well known that the prices of discrete path dependent options are highly sensitive to monitoring frequency (say, daily monitored barrier options may be 50% or 100% higher than those of the weekly monitored counterparts even under non-extreme scenario). Though analytical approximation formulas are available for barrier options and lookback options for a few common underlying asset price processes, like Geometric Brownian motions and jump-diffusion processes (Broadie *et al.*, 1997; Broadie *et al.*, 1999; Dia and Lamberton, 2011), accuracy of the analytic approximation formulas may deteriorate significantly, like what is shown in a barrier option when the asset price is close to the knock-out barrier. A review of

¹Correspondence author; email: maykwok@ust.hk; fax number: 852-2358-1643

various analytical approximation methods and numerical schemes for pricing discrete barrier and lookback options can be found in Kou (2008).

There have been continual research efforts in the past two decades to explore effective computational algorithms for pricing discrete barrier options, lookback options and Bermudan options. Under the assumption of Geometric Brownian motion (GBM) for the underlying asset price process, one may derive closed form analytical price formulas for discrete barrier and lookback options that are expressed in terms of multivariate normal distribution functions, where the dimension equals the number of monitoring instants n (Heynen and Kat, 1995). The numerical evaluation of these high-dimensional multivariate normal distribution functions is a daunting task. By observing that the inverse of the Brownian correlation matrix has a simple tridiagonal structure, Tse *et al.* (2001) develop an effective numerical algorithm that is quadratic order in the number of spatial points p in each integral evaluation. That is, the order of complexity is $O(np^2)$ instead of $O(np^n)$ in direct valuation of the n -dimensional multivariate normal distribution functions. Alternatively, the formulation of discrete barrier and lookback options can be expressed as a convolution of density functions over successive monitoring instants. Based on the duality property of random walks, AitSahlia and Lai (1998) develop the recursive integration procedure for pricing discrete lookback options. Using the convolution integral approach together with the elegant use of the fast Gauss transform (involving the use of the Hermite functions in the expansion of the exponential kernel), Broadie and Yamamoto (2005) develop efficient numerical algorithms that have computational complexity of $O(np)$ or linear order in the number of spatial points in each integral evaluation. Their algorithms are applicable for pricing discrete barrier and lookback options under GBM and Merton's lognormal jump-diffusion model. For other types of underlying price processes, like the CEV and variance gamma processes, Fusai and Recchioni (2007) develop the quadrature methods for pricing discrete barrier options that exhibit computational complexity of $O(np^2)$. Petrella and Kou (2004) use the renowned Spitzer formula to derive the Laplace transforms of both discrete barrier and lookback options via a recursive algorithm that involves analytical formulas of vanilla European options. The Laplace transforms can be inverted numerically to obtain the desired option values. Fusai *et al.* (2006) show that valuation problems of discrete barrier options under GBM can be reduced to the numerical solution of the Wiener-Hopf type integral equation of the second kind. Atkinson and Fusai (2007) show that the solution procedure via the Wiener-Hopf integral equation for pricing discrete lookback options can be related to the method that uses the Spitzer identity.

The other class of numerical methods are the finite difference schemes and lattice tree type algorithms. Zvan *et al.* (2000) present various types of implicit finite difference schemes for pricing discrete barrier options. Andreasen (1998) proposes a dimension reduction technique via numeraire change for pricing discrete lookback options under GBM. The numerical procedure involves finite difference solution of a sequence of one-dimensional partial differential equations. Duan *et al.* (2003) propose a Markov chain method for pricing discrete barrier options under constant and time-varying volatilities, where a time homogeneous Markov chain is used to approximate the underlying asset price process.

When we consider pricing discrete path dependent options under Lévy processes, it is natural to perform valuation of the option values in the Fourier domain. This is because the characteristic function (Fourier transform of the density function) of the Lévy process generally admits analytical closed form representation while that of the density function itself may not be readily available. A review of the fast Fourier transform (FFT) algorithms for pricing options can be found in Kwok *et al.* (2012). Jackson *et al.* (2008) propose the Fourier space time-stepping methods for pricing discrete barrier and American options. In their time-stepping procedure, after the Fourier time-stepping integration across successive

monitoring instants, one has to perform Fourier inversion back to the real domain at each monitoring instant to check for the knock-out condition or optimal early exercise decision. To circumvent this source of computational inconvenience, Feng and Linetsky (2008) propose the fast Hilbert transform method that computes a sequence of Hilbert transforms at all discrete monitoring instants and performs one final Fourier inversion to obtain the option price. The key ingredient in the fast Hilbert transform method is that multiplying a function by the indicator function associated with the barrier feature in the real domain corresponds to taking Hilbert transform in the Fourier domain. The fast Hilbert transform method is extended to computing exponential moments of the discrete maximum of a Lévy process and lookback options (Feng and Linetsky, 2009), as well as pricing Bermudan options under Lévy processes (Feng and Lin, 2013). The Fourier transform methods are also applied to pricing barrier and Bermudan options under the Heston model of stochastic volatility (Fang and Oosterlee, 2011; Zhylyevskyy, 2010).

In this paper, we apply the fast Hilbert transform method for pricing discrete barrier options and Bermudan options under time-changed Lévy processes. We extend the earlier fast Hilbert transform algorithms (Feng and Linetsky, 2008; Feng and Lin, 2013) by applying an appropriate interpolation based quadrature rule for numerical integration in the dimension of log-activity rate of stochastic time change. We manage to extend the method to finding the fair value of a finite dividend-ruin model with the upper reflecting (dividend) barrier and lower absorbing (ruined) barrier. It is well known that the time-changed Lévy models nest the popular Heston stochastic volatility model. For pricing Bermudan options under the Heston model, our algorithm is shown to be highly accurate and achieves better computational efficiency compared to the Fourier cosine method (Fang and Oosterlee, 2011).

This paper is organized as follows. In the next section, we review some mathematical preliminaries on time-changed Lévy processes and Hilbert transform. We generalize the time-changed Lévy processes to include leverage effect and show how to relate the Heston stochastic volatility model to the time-changed Lévy process with leverage. In Section 3, we consider pricing of the discretely monitored finite time dividend-ruin models under time-changed Lévy processes. We illustrate how the fast Hilbert transform algorithm can be used to deal with the reflecting (dividend) barrier condition and consider the extension of Feng-Linetsky's algorithm to include the adoption of the Gauss-Legendre quadrature rule for numerical integration in the log-activity rate dimension. In Section 4, we consider pricing of the Bermudan options under time-changed Lévy processes. Specifically, we construct the numerical procedure for the determination of the critical asset prices with regard to early exercise of the Bermudan option. We also consider various numerical procedures that are adopted to achieve optimal computational efficiency in the fast Hilbert transform algorithm, like including an effective implementation of the matrix-vector multiplication in Toeplitz matrices. In Section 5, we present the numerical tests that were performed to assess accuracy and computational efficiency of the fast Hilbert transform algorithms for pricing various discrete path dependent products under different time-changed Lévy processes. Conclusive remarks are presented in the last section.

2 Preliminaries on time-changed Lévy processes and Hilbert transform

The literature on Lévy processes has been quite voluminous. A good review of various types of Lévy security return models can be found in Wu (2008). Pricing models of financial derivatives based on Lévy processes have become highly popular in recent years since Lévy

processes can generate different independent and identically (i.i.d) return innovation distributions. One can specify a Lévy process with the increments of the process matching any given distribution. However, Lévy processes cannot capture the following salient features of common stock price processes: stochastic volatility, stochastic risk reversal (skewness) and stochastic correlation.

Three different approaches have been proposed in the literature to model stochastic volatility. An intuitive approach is via a regime-switching model. For example, Kim *et al.* (2012) propose a stochastic volatility model with a Lévy driving process where the stochastic volatility is defined by a continuous Markov chain. Also, we can incorporate a time-series model to account for volatility. The typical time-series model is the GARCH model that takes into account several stylized facts, such as volatility clustering. Unfortunately, inefficiency in numerical implementation is the main drawback of the GARCH model. The last approach is to capture stochastic volatility via time changes in Lévy processes. Time-changed Lévy processes provide a flexible framework, since one can use the Lévy process to generate jumps, capture the stochastic volatility by the random time change, and introduce the leverage effect. Another main advantage in the adoption of time-changed Lévy processes in security return models is their nice analytical tractability and high efficiency in implementation.

2.1 Time-changed Lévy processes

Let X_t be a Lévy process with filtration \mathcal{F}_t , whose characteristic function is given by the Lévy-Khintchine theorem. In the context of a time-changed Lévy process, X_t is referred as the base process. We let T_t be a non-negative, non-decreasing right-continuous process with left limits such that for each fixed t the random variable T_t is a stopping time with respect to \mathcal{F}_t . The family of the stopping times T_t define the corresponding random time change and the resulting process

$$M_t = X_{T_t} \tag{2.1}$$

is called a time-changed Lévy process. There are different methods for choosing a time change that is suitable for various types of financial security return models. The two most popular approaches are the subordinators and absolutely continuous time changes.

Subordinators are non-decreasing Lévy processes. They are pure jump processes of possibly infinite activity plus a deterministic linear drift. Note that many popular Lévy processes can be generated as a Brownian motion time-changed by an independent subordinator. For example, the Normal Tempered Stable process can be regarded as a Brownian motion time-changed by a tempered stable subordinator while the variance gamma process can be represented as a Brownian motion subject to a gamma subordinator.

Another important type of time changes are given by the continuous time change of the form $T_t = \int_0^t v_s ds$, where v_t is the instantaneous (business) activity rate. Intuitively, one can regard t as the calendar time and T_t as the business time at t . A more active business day as captured by a higher activity rate would imply a higher volatility. While the instantaneous activity rate process v_t is allowed to have jumps, T_t remains to be continuous with time according to the above definition. Note that the jumps in v_t are required to be nonnegative in order to guarantee the nondecreasing property of T_t . The main advantage of the choice of continuous time change is that it leads to security return models that are analytically tractable.

Martingale condition

By the Lévy-Khintchine theorem and under an equivalent martingale measure Q , a general

Lévy process X_t has its characteristic function represented in the following analytic form

$$\phi_t(\xi) = E_Q[e^{i\xi X_t}] = e^{-t\psi_X(\xi)} = \exp\left(-t\left[\frac{\sigma^2}{2}\xi^2 - i\mu\xi + \int_{\mathbb{R}}(1 - e^{i\xi y} + i\xi y \mathbf{1}_{|y|\leq 1}) \Pi(dy)\right]\right), \quad (2.2)$$

where the triplet (μ, σ^2, Π) characterizes the drift, the variance of the diffusion component, and the pure jump component of a Lévy process. Here, $\psi_X(\xi)$ is known as the Lévy characteristic exponent. We define

$$\mathcal{L}_X = \{\theta \in \mathbb{R} : E[e^{-\theta X_t}] < \infty, t > 0\},$$

which can be shown to be an interval containing the origin with endpoints $\lambda_- < 0$ and $\lambda_+ > 0$ (Sato, 1999; Küchler and Sorensen, 1997). To guarantee that e^{X_t} is a martingale under Q , the corresponding martingale condition is given by

$$E_Q[e^{X_t}] = \phi_t(-i) = e^{X_0},$$

so that $\phi_t(-i) = 1$. Later, we drop the subscript “ Q ” in the expectation operator E_Q for brevity. The martingale condition leads to the following condition on the drift parameter μ of the Lévy process

$$\mu = -\frac{\sigma^2}{2} + \int_{\mathbb{R}}(1 - e^y + y \mathbf{1}_{|y|\leq 1}) \Pi(dy). \quad (2.3)$$

In order that the martingale condition holds, it is necessary to have $\theta = -1 \in \mathcal{L}_X$. As a result, we have to assume $[-1, 0] \subset (\lambda_-, \lambda_+)$.

Since a continuous time change does not affect the martingale property, it follows that $e^{X_{T_t}}$ remains to be a martingale. In this paper, we model the dynamics of the underlying log-asset return by this type of time-changed Lévy process. More precisely, the log-asset return process is modeled as a time-changed Lévy process of the form

$$S_t = S_0 e^{rt} e^{M_t} = S_0 e^{rt} e^{X_{T_t}}. \quad (2.4)$$

For nice analytical tractability, we assume X_t and T_t to be independent. Under the independence assumption, together with the given characteristic function of T_t , we can obtain the closed form for the characteristic function of the time-changed Lévy process without invoking change of measures. Also, we can avoid the nuisance of estimating the correlation coefficient between X_t and T_t , a procedure that may not be straightforward in most practical cases.

Cox-Ingersoll-Ross process as the activity rate process

While there are many different choices for a stochastic process that serves as the activity rate process in stochastic time change, we confine our choice to the Cox-Ingersoll-Ross (CIR) process in this paper. A process v_t is said to be a CIR process or a square-root process if its dynamics is governed by the following stochastic differential equation

$$dv_t = \lambda(\bar{v} - v_t)dt + \eta\sqrt{v_t} dW_t^v. \quad (2.5)$$

Note that the singularity of the diffusion coefficient at the origin disallows subsequent non-negative value for v_t once v_t starts with an initial positive value. Actually, the occurrence of square root of v_t in the diffusion coefficient would preclude negative value for v_t . The CIR process has the mean reversion property exhibited in the drift term and the parameter \bar{v} has the usual interpretation as the mean reversion level. The corresponding continuous CIR clock with v_t as the activity rate process is given by the following time change integral

$$T_t = \int_0^t v_s ds. \quad (2.6)$$

Feller condition

When the Feller condition, $2\lambda\bar{v} \geq \eta^2$, is satisfied, the origin becomes inaccessible to the CIR process v_t . This would guarantee that v_t stays strictly positive. Unfortunately, the CIR model parameters obtained from the calibration of market data may fail to satisfy the Feller condition. When the Feller condition fails, the cumulative distribution of the variance modeled by the CIR process may show an almost singular behavior near the origin (Andersen, 2008). The origin is accessible by v_t and strongly reflecting. More specifically, the density of variance v_t grows extremely fast in the left tail. The phenomenon in the left tail may give rise to significant errors in the integration based option pricing methods, where a finite truncation of the integration range for the variance is adopted. To resolve this difficulty, Fang and Oosterlee (2011) propose to transform the density function from the variance domain to the log-variance domain by defining $\gamma_t = \ln v_t$. We follow a similar approach to deal with this potential problem of singular behavior since the Feller condition may fail. In our subsequent exposition, the variable is taken to be the log-activity rate as defined by $\gamma_t = \ln v_t$. Since negative value for v_t is precluded in the CIR process, the log-activity rate γ_t is well defined. In Appendix A, we provide the theoretical justification to explain why computational convenience can be achieved when we adopt the transformation from v_t to γ_t . Also, the characteristic function and other related properties of the CIR process are presented.

Leverage in time-changed Lévy processes

We consider the class of time-changed Lévy processes with leverage by adding the leverage term cv_t , where

$$L_t = X_{T_t} + cv_t. \quad (2.7)$$

Here, X_t and T_t are assumed to be independent and a scalar multiple c of the activity rate v_t is added to the time-changed Lévy process. Fortunately, nice analytical tractability is retained since the conditional moment generating function of $L_t - L_s$ admits the following structure

$$\begin{aligned} E[e^{w(L_t - L_s)} | \mathcal{F}_s, \gamma_t] &= e^{wc(v_t - v_s)} E[e^{w(X_{T_t} - X_{T_s})} | \mathcal{F}_s, \gamma_t] \\ &= e^{wc(v_t - v_s)} E\left[E[e^{w(X_{T_t} - X_{T_s})} | T_t - T_s, \mathcal{F}_s, \gamma_t] | \mathcal{F}_s, \gamma_t\right] \\ &= e^{wc(e^{\gamma_t} - e^{\gamma_s})} E\left[e^{-\psi_X(-iw)(T_t - T_s)} | \mathcal{F}_s, \gamma_t\right] \\ &= e^{wc(e^{\gamma_t} - e^{\gamma_s})} \Phi(i\psi_X(-iw); \gamma_t, \gamma_s), \end{aligned} \quad (2.8)$$

where $\Phi(\xi; \gamma_t, \gamma_s) = E[e^{i\xi \int_s^t v_u du} | \gamma_t, \gamma_s]$ is the conditional characteristic function of the time-integrated activity rate process $\int_s^t v_u du$. As an example, the corresponding $\Phi(\xi; \gamma_t, \gamma_s)$ of the CIR activity rate process is given by Eq. (A.3) in Appendix A.

Heston stochastic volatility model

The correlated stochastic processes S_t and v_t with correlation coefficient ρ under the Heston stochastic volatility model are governed by

$$\begin{aligned} \frac{dS_t}{S_t} &= rdt + \sqrt{v_t} dW_t, \\ dv_t &= \lambda(\bar{v} - v_t)dt + \eta\sqrt{v_t} dW_t^v. \end{aligned} \quad (2.9)$$

where $E[dW_t dW_t^v] = \rho dt$. The log-asset return Y_t can be expressed as a time-changed Lévy process with leverage as follows

$$Y_t = \ln \frac{S_t}{S_0} = rt + \widetilde{W}_{T_t} - \frac{1}{2}T_t,$$

where $d\widetilde{W}_t$ and $\sqrt{v_t} dW_t$ are equal in distribution. Fortunately, the log-asset return conditional on v_t can be expressed in terms of X_{T_t} as follows

$$Y_t|v_t = (r - \frac{\rho\lambda\bar{v}}{\eta})t + X_{T_t} + \frac{\rho}{\eta}(v_t - v_0),$$

where $X_t \sim N((\frac{\rho\lambda}{\eta} - \frac{1}{2})t, (1 - \rho^2)t)$. The corresponding characteristic exponent is given by

$$\psi_X(\xi) = (\frac{1}{2} - \frac{\rho\lambda}{\eta})i\xi + \frac{1}{2}(1 - \rho^2)\xi^2.$$

The conditional moment generating function of the difference of the log-asset return is defined by

$$\Psi(w; \gamma_t, \gamma_s) = E[e^{w(Y_t - Y_s)} | \mathcal{F}_s, \gamma_t].$$

Once $Y_t|v_t$ and $\psi_X(\xi)$ are known for the Heston model (nested within the class of time-changed Lévy processes with leverage), the analytic representation of $\Psi(w; \gamma_t, \gamma_s)$ is given by [see Eq. (2.8)]

$$\Psi(w; \gamma_t, \gamma_s) = e^{w\{r(t-s) + \frac{\rho}{\eta}[e^{\gamma_t} - e^{\gamma_s} - \lambda\bar{v}(t-s)]\}} \Phi(-iw(\frac{\rho\lambda}{\eta} - \frac{1}{2}) - \frac{1}{2}iw^2(1 - \rho^2); \gamma_t, \gamma_s). \quad (2.10)$$

We have suppressed the dependency of $\Psi(w; \gamma_t, \gamma_s)$ on t and s for notational convenience.

2.2 Hilbert transform

Let Ω be an arbitrary measure space with positive measure μ . For $0 < p < \infty$, we let f be a complex measurable function on Ω and define the norm by $\|f\|_p = \{\int_{\Omega} |f|^p d\mu\}^{1/p}$. The vector space $L^p(\mu)$ consists of all f for which $\|f\|_p < \infty$. If μ is a Lebesgue measure on \mathbb{R} , we write $L^p(\mathbb{R})$ instead of $L^p(\mu)$. For any $f \in L^p(\mathbb{R})$, $1 \leq p < \infty$, the Hilbert transform of f is well defined by the Cauchy principal value integral (King, 2009)

$$\mathcal{H}f(x) = \frac{1}{\pi} PV \int_{\mathbb{R}} \frac{f(y)}{x - y} dy. \quad (2.11)$$

For $1 < p < \infty$ and $g \in L^p(\mathbb{R})$, the following parity relation holds for the primitive function $f(x)$ and its Hilbert transform $g(x)$, where

$$g(x) = \frac{1}{\pi} PV \int_{\mathbb{R}} \frac{f(y)}{x - y} dy, \quad f(x) = -\frac{1}{\pi} PV \int_{\mathbb{R}} \frac{g(y)}{x - y} dy.$$

Recall that for any $f \in L^p(\mathbb{R})$, $1 \leq p < \infty$, its Fourier transform $\widehat{f} = \mathcal{F}f \in L^q(\mathbb{R})$ with $\frac{1}{p} + \frac{1}{q} = 1$.

The Hilbert transform is closely related to the Fourier transform. For $1 < p < \infty$, the following relationship holds for any $f \in L^p(\mathbb{R})$

$$\mathcal{F}(\text{sgn} \cdot f)(\xi) = i\mathcal{H}\widehat{f}(\xi), \quad (2.12)$$

where $\text{sgn}(x)$ is the sign function, and $H\widehat{f} \in L^q(\mathbb{R})$ with $\frac{1}{p} + \frac{1}{q} = 1$. For the special case $p = 1$, we require $\widehat{f} \in L^1(\mathbb{R})$ so that the above relationship holds. Recall that the indicator function $\mathbf{1}_{(0, \infty)}$ is related to the sign function by

$$\mathbf{1}_{(0, \infty)} = \frac{1}{2}[1 + \text{sgn}(x)].$$

As a result, we obtain the following formula that relates the Fourier transform of a function multiplied by the indicator function to the Hilbert transform of the Fourier transform function

$$\mathcal{F}(\mathbf{1}_{(0,\infty)} \cdot f)(\xi) = \frac{1}{2}\widehat{f}(\xi) + \frac{i}{2}\mathcal{H}\widehat{f}(\xi). \quad (2.13)$$

This is one of the most crucial formulas in the construction of the fast Hilbert transform algorithm. Furthermore, we can extend the above relation to other types of intervals, like (l, ∞) and $(l, u]$, using some appropriate shifting translations. For any constant parameter values l and u , where $l < u$, we have

$$\mathcal{F}(\mathbf{1}_{(l,\infty)} \cdot f)(\xi) = \frac{1}{2}\widehat{f}(\xi) + \frac{i}{2}e^{i\xi l}\mathcal{H}(e^{-i\eta l}\widehat{f}(\eta))(\xi), \quad (2.14a)$$

$$\mathcal{F}(\mathbf{1}_{(l,u]} \cdot f)(\xi) = \int_{-\infty}^{\infty} \widehat{f}(\eta) e^{\frac{i}{2}(\xi-\eta)(l+u)} \frac{\sin\frac{(\xi-\eta)(u-l)}{2}}{\pi(\xi-\eta)} d\eta. \quad (2.14b)$$

Another attractive property of the Hilbert transform is that it can be expanded based on the Sinc expansion of an analytic function (Feng and Linetsky, 2008), where

$$\mathcal{H}f(x) = \frac{1}{\pi}PV \int_{\mathbb{R}} \frac{f(y)}{x-y} dy = \sum_{m=-\infty}^{\infty} f(mh) \frac{1 - \cos\frac{\pi(x-mh)}{h}}{\frac{\pi(x-mh)}{h}}, \quad h > 0. \quad (2.15)$$

Here, h is some fixed discretization step.

3 Dividend-ruin models under time-changed Lévy processes

Leung *et al.* (2008) propose the finite time dividend-ruin model where the firm pays out dividends to its shareholders at some upstream barrier according to a dividend barrier strategy and becomes ruined when the firm asset value hits some downstream default threshold. Analytical solution to the value function of the restricted firm asset value process can be derived under the assumption of the Geometric Brownian motion and continuous monitoring of the upper reflecting (dividend) barrier and lower absorbing (ruined) barrier. In this section, we would like to consider pricing of the discrete dividend-ruin models under time-changed Lévy processes using the fast Hilbert transform algorithm.

Let the current time be $t_0 = 0$, and denote the set of monitoring times in the finite time dividend-ruin model by $\mathcal{T} = \{t_0, t_1, \dots, t_N\}$, where $t_N = T$ is the maturity. Though the time intervals between successive monitoring times may not be uniform in general, without loss of generality, we assume a uniform monitoring interval Δ to simplify the presentation of the model. For uniform time intervals, we write $t_k = k\Delta$, $k = 0, 1, \dots, N$.

Model formulation: reflecting and absorbing barriers

We consider the dividend-ruin model where the logarithm of the unrestricted firm asset value process A_t is modeled as a time-changed Lévy process. Under a risk neutral measure Q , we assume A_t to follow the following dynamics

$$A_t = e^{Y_t} = e^{rt} e^{X_{T_t}},$$

where X_{T_t} is a time-changed Lévy process. We write $Y_0 = \ln A_0$, where A_0 is the firm asset value at time t_0 . The liability level L (lower absorbing barrier), visualized as the knock-out barrier of the firm asset value process, is monitored at a discrete set of times \mathcal{T} . On the

other hand, the firm may pay out dividends to its shareholders according to a dividend barrier strategy at the upper barrier B on a monitoring date. More precisely, whenever the firm asset value rises to the level B on a monitoring date, the excess amount will be paid out as dividend. Under such dividend barrier strategy, the restricted firm asset value on a monitoring date can never go above the reflecting barrier B . Subject to the possibilities of ruin and dividend payouts on monitoring dates, the restricted firm asset value process is seen to include both the discrete lookback and barrier features.

Let \underline{A}_0^t and \overline{A}_0^t denote the realized minimum value and maximum value of the firm asset value process within $[0, t]$ under discrete monitoring. Suppose $j = \max\{i : t_i \leq t\}$, we have

$$\underline{A}_0^t = \min\{A_{t_0}, A_{t_1}, \dots, A_{t_j}\} \text{ and } \overline{A}_0^t = \max\{A_{t_0}, A_{t_1}, \dots, A_{t_j}\}. \quad (3.1)$$

Over the finite period $[0, t]$, conditional on survival and adoption of the dividend barrier strategy, the fraction of the firm asset remaining is given by $\min(1, \frac{B}{\overline{A}_0^t})$. Accordingly, it is convenient to define the non-ruined modified firm asset value \widehat{A}_t at time t by

$$\widehat{A}_t = A_t \min(1, \frac{B}{\overline{A}_0^t}). \quad (3.2)$$

Note that \overline{A}_0^t may exhibit jump across a monitoring date when a new discrete maximum of the firm asset value process is realized, so does \widehat{A}_t . Likewise, we define the discrete minimum value of \widehat{A}_t over the interval $[T_1, T_2]$ by

$$\underline{\widehat{A}}_{T_1}^{T_2} = \min_{T_1 \leq t_j \leq T_2} \widehat{A}_{t_j}.$$

Let \widetilde{A}_t denote the restricted firm asset value process with the two-sided discretely monitored reflecting and absorbing barriers. The restricted firm asset value at time T is given by

$$\widetilde{A}_T = \widehat{A}_T \mathbf{1}_{\{\underline{\widehat{A}}_0^T > L\}}. \quad (3.3)$$

The event $\{\underline{\widehat{A}}_0^T \leq L\}$ captures the occurrence of ruin when the non-ruined modified firm asset value \widehat{A}_t falls at or below L at any monitoring time instant over $[0, T]$.

Value function of the firm asset value process

We are interested in computing the time- t value function of the firm asset value with discretely monitored lower ruined barrier L and upper dividend barrier B . For pricing under time-changed Lévy processes, recall that v_t denotes the activity rate of stochastic time change. In this paper, we take v_t to be the CIR process as defined in Eq. (2.5). We write $\gamma_t = \ln v_t$, where γ_t is the log-activity rate, so the value function depends on γ_t as well. Let $V_{in}(A_t, \gamma_t, t; \underline{\widehat{A}}_0^t, \overline{\widehat{A}}_0^t)$ denote the in-progress time- t value function of the firm asset value with dependence on the state variables A_t and γ_t , together with the path dependent state variable $\underline{\widehat{A}}_0^t$ and $\overline{\widehat{A}}_0^t$. By virtue of risk neutral valuation, V_{in} is given by the expected present value of the terminal restricted firm asset value

$$V_{in}(A_t, \gamma_t, t; \underline{\widehat{A}}_0^t, \overline{\widehat{A}}_0^t) = E_t[e^{-r(T-t)} \widetilde{A}_T]. \quad (3.4)$$

We define $V_0(A_t, \gamma_t, t)$ as the “initiation-state” value function corresponding to the state where A_t has never reached either the lower absorbing barrier or the upper reflecting barrier at earlier monitoring times $\mathcal{T}_t = \{t_0, \dots, t_j\}$, where $j = \max\{i : t_i \leq t\}$. The notion of “initiation-state” value function has been commonly used in pricing lookback options.

Coined as the “initiation state” value function, $V_0(A_t, \gamma_t, t)$ has no dependence on \widehat{A}_0^t and \overline{A}_0^t . It is instructive to establish the following relation between V_{in} and V_0 (Leung *et al.*, 2008):

$$\begin{aligned} V_{in}(A_t, \gamma_t, t; \widehat{A}_0^t, \overline{A}_0^t) &= \begin{cases} V_0(\frac{B}{\widehat{A}_0^t} A_t, \gamma_t, t) & \text{if } \widehat{A}_0^t > L \text{ and } \overline{A}_0^t > B \\ V_0(A_t, \gamma_t, t) & \text{if } \widehat{A}_0^t > L \text{ and } \overline{A}_0^t \leq B \\ 0 & \text{if } \widehat{A}_0^t \leq L \end{cases} \quad (3.5) \\ &= V_0(\widehat{A}_t, \gamma_t, t) \mathbf{1}_{\{\widehat{A}_0^t > L\}}. \end{aligned}$$

In our subsequent exposition, it is more convenient to use $Z_t = \ln \widehat{A}_t$ as the state variable and write $V(Z_t, \gamma_t, t) = V_0(\widehat{A}_t, \gamma_t, t)$, $l = \ln L$ and $b = \ln B$. Next, we would like to develop the fast Hilbert transform algorithm to compute $V(Z_t, \gamma_t, t)$.

Jump condition on the value function across a monitoring date

Let t_k^- and t_k^+ represent the time instant immediately before and after the monitoring date t_k , $k = 1, 2, \dots, N$. Since there is no cash flow to the holder of the firm asset across a monitoring date, the value function should remain the same at the instants right before and after any monitoring date t_k . Suppose $Z_{t_k^-} > b$, then $Z_{t_k^+}$ is set to become b . This jump condition across the monitoring time instant t_k models the fraction of firm asset value lost to dividend payout and the resulting firm asset value is reduced to the dividend barrier B due to the dividend barrier strategy. On the other hand, Z_t remains continuous across t_k when $Z_{t_k^-} \leq b$. The ruin feature can be modeled by the indicator function $\mathbf{1}_{\{l < Z_{t_k^-} \leq b\}}$ so that the value function becomes zero when $Z_{t_k^-} \leq l$. By following a similar approach used by Andreasen (1998) for pricing discrete lookback options, the jump condition of the value function is given by

$$V(Z_{t_k^-}, \gamma_{t_k}, t_k^-) = V(Z_{t_k^-}, \gamma_{t_k}, t_k^+) \mathbf{1}_{\{l < Z_{t_k^-} \leq b\}} + V(b, \gamma_{t_k}, t_k^+) \mathbf{1}_{\{Z_{t_k^-} > b\}}. \quad (3.6a)$$

We initiate our time stepping calculations at the instant right before the maturity date t_N . The terminal condition for the value function is set to be

$$V(Z_{t_N^-}, \gamma_{t_N}, t_N^-) = e^{Z_{t_N^-}} \mathbf{1}_{\{l < Z_{t_N^-} \leq b\}} + B \mathbf{1}_{\{Z_{t_N^-} > b\}}. \quad (3.6b)$$

Time-stepping calculations between successive monitoring dates

The martingale pricing theory gives the following risk neutral valuation formula

$$V(Z_{t_k^+}, \gamma_{t_k}, t_k^+) = e^{-r\Delta} E[V(Z_{t_{k+1}^-}, \gamma_{t_{k+1}}, t_{k+1}^-) | \mathcal{F}_{t_k^+}],$$

where $\Delta = t_{k+1} - t_k$. By the tower property and conditional on the log-activity rate process $\gamma_{t_{k+1}}$ at time t_{k+1} , it follows that

$$V(Z_{t_k^+}, \gamma_{t_k}, t_k^+) = e^{-r\Delta} E \left[E[V(Z_{t_{k+1}^-}, \gamma_{t_{k+1}}, t_{k+1}^-) | \mathcal{F}_{t_k^+}, \gamma_{t_{k+1}}] | \mathcal{F}_{t_k^+} \right].$$

This expectation formula dictates that the time-stepping calculations between successive monitoring dates for the value function of the restricted firm asset value under time-changed Lévy processes can be expressed as a two-dimensional expectation integral. The outer expectation integral involves integration over the density function $p_\gamma(\gamma_{t_{k+1}} | \gamma_{t_k})$, which has analytic closed form if the activity rate process v_t is chosen to be the CIR process [see Eq. (A.2)]. To evaluate the two-dimensional expectation integral between successive monitoring dates, we

apply an interpolation based quadrature rule for the numerical valuation of the outer expectation integral and the Fourier transform method for the inner expectation integral. Across a monitoring date, due to the the jump condition associated with the discretely monitored dividend-ruin model as exemplified by Eqs. (3.6a) and (3.6b), we can take advantage of the fast Hilbert transform method to deal with the barrier feature.

Numerical quadrature rule

As the first step, we apply an appropriate J -point quadrature integration rule (like the Gauss-Legendre quadrature or composite trapezoidal rule) to effect numerical evaluation of the outer expectation integral. By performing discretization along the dimension of $\gamma_{t_{k+1}}$ at the discrete nodes ζ_j , $j = 1, 2, \dots, J$, we obtain

$$V(Z_{t_k^+}, \gamma_{t_k}, t_k^+) \approx e^{-r\Delta} \sum_{j=1}^J w_j p_\gamma(\zeta_j | \gamma_{t_k}) E \left[V(Z_{t_{k+1}^-}, \gamma_{t_{k+1}}, t_{k+1}^-) | \mathcal{F}_{t_k^+}, \gamma_{t_{k+1}} = \zeta_j \right], \quad (3.7)$$

where w_j is the weight at the quadrature node ζ_j , $j = 1, 2, \dots, J$.

CONV method

To perform the inner expectation calculations, we adopt the CONV method that is commonly used in Fourier option pricing algorithms (Lord *et al.*, 2008; Kwok *et al.*, 2012). In a typical Fourier option pricing algorithm, in order to guarantee that the Fourier transforms are well defined, it is necessary to introduce a properly chosen exponential damping factor. Let $w = \alpha + i\beta$, where α is a constant. At $\gamma_{t_{k+1}} = \zeta_j$ and $Z_{t_{k+1}^-} = x$, we define $V_\alpha(x, \zeta_j, t_{k+1}^-) = e^{\alpha x} V(x, \zeta_j, t_{k+1}^-)$, where $e^{\alpha x}$ is some appropriate exponential damping factor for the value function $V(x, \zeta_j, t_{k+1}^-)$ at all nodes ζ_j . The parameter α is chosen to insure the existence of the generalized Fourier transform of $V(x, \zeta_j, t_{k+1}^-)$. The generalized Fourier transform of $V(x, \zeta_j, t_{k+1}^-)$ is defined by

$$\hat{V}_\alpha(\beta, \zeta_j, t_{k+1}^-) = \int_{-\infty}^{\infty} e^{w x} V(x, \zeta_j, t_{k+1}^-) dx = \int_{-\infty}^{\infty} e^{i\beta x} V_\alpha(x, \zeta_j, t_{k+1}^-) dx.$$

By virtue of the renowned Parseval relation in Fourier transform, we have

$$\begin{aligned} E[V(Z_{t_{k+1}^-}, \gamma_{t_{k+1}}, t_{k+1}^-) | \mathcal{F}_{t_k^+}, \gamma_{t_{k+1}} = \zeta_j] &= \int_{-\infty}^{\infty} V(x, \zeta_j, t_{k+1}^-) p(x | \mathcal{F}_{t_k^+}, \gamma_{t_{k+1}} = \zeta_j) dx \\ &= \frac{1}{2\pi} \int_{-\infty}^{\infty} \hat{V}_\alpha(\beta, \zeta_j, t_{k+1}^-) \check{p}(w | \mathcal{F}_{t_k^+}, \gamma_{t_{k+1}} = \zeta_j) d\beta. \end{aligned} \quad (3.8)$$

Here, $\check{p}(w | \mathcal{F}_{t_k^+}, \gamma_{t_{k+1}} = \zeta_j) = E[e^{-w x} | \mathcal{F}_{t_k^+}, \gamma_{t_{k+1}} = \zeta_j]$ is visualized as the generalized inverse Fourier transform of the conditional density function $p(x | \mathcal{F}_{t_k^+}, \gamma_{t_{k+1}} = \zeta_j)$ of $Z_{t_{k+1}^-}$. Over the time period (t_k^+, t_{k+1}^-) , there is no dividend payment and ruin does not occur. Based on Eq. (3.2), the dynamics of the unrestricted and non-ruined modified firm asset processes are the same over (t_k^+, t_{k+1}^-) , and we have $Z_{t_{k+1}^-} - Z_{t_k^+} = Y_{t_{k+1}} - Y_{t_k}$. We can rewrite $\check{p}(w | \mathcal{F}_{t_k^+}, \gamma_{t_{k+1}} = \zeta_j)$ into the following representation

$$\check{p}(w | \mathcal{F}_{t_k^+}, \gamma_{t_{k+1}} = \zeta_j) = e^{-w Z_{t_k^+}} E[e^{-w(Y_{t_{k+1}} - Y_{t_k})} | \mathcal{F}_{t_k^+}, \gamma_{t_{k+1}} = \zeta_j]. \quad (3.9)$$

Recall $\Psi(w; \gamma_t, \gamma_s) = E[e^{w(Y_t - Y_s)} | \mathcal{F}_s, \gamma_t]$, we attempt to relate $\Psi(w; \gamma_t, \gamma_s)$ to the characteristic

function of X_t . By the tower property, we have

$$\begin{aligned}
\Psi(w; \gamma_t, \gamma_s) &= E\left[E[e^{w(Y_t - Y_s)} | \mathcal{F}_s, \gamma_t, T_t - T_s] | \mathcal{F}_s, \gamma_t\right] \\
&= E\left[E[e^{w(Y_t - Y_s)} | T_t - T_s] | \mathcal{F}_s, \gamma_t\right] \\
&= e^{wr(t-s)} E[e^{-\psi_X(-iw)(T_t - T_s)} | \mathcal{F}_s, \gamma_t] \\
&= e^{wr(t-s)} \Phi(i\psi_X(-iw); \gamma_t, \gamma_s).
\end{aligned} \tag{3.10}$$

It is worthwhile to mention that $\Psi(w; \gamma_t, \gamma_s)$ admits the closed form representation when incorporating the leverage effect, which has been derived in the previous section. Combining Eqs. (3.8), (3.9) and (3.10), we may express the inner expectation integral at $\gamma_{t_{k+1}} = \zeta_j$ as the following inverse Fourier transform representation

$$E[V(Z_{t_{k+1}}^-, \gamma_{t_{k+1}}, t_{k+1}^-) | \mathcal{F}_{t_k}^+, \gamma_{t_{k+1}} = \zeta_j] = \frac{1}{2\pi} \int_{-\infty}^{\infty} e^{-wZ_{t_k}^+} \hat{V}_\alpha(\beta, \zeta_j, t_{k+1}^-) \Psi(-w; \zeta_j, \gamma_{t_k}) d\beta. \tag{3.11}$$

Here, we have set $\gamma_{t_{k+1}} = \zeta_j$ in the conditional moment generating function $\Psi(w; \gamma_{t_{k+1}}, \gamma_{t_k})$.

Summary of the computational procedures

Given $N + 1$ discrete monitoring dates, where $\mathcal{T} = \{t_k | k = 0, 1, \dots, N\}$ with $t_N = T$, the sequential computational steps associated with numerical evaluation of the two-dimensional expectation integral are summarized as follows:

- (i) The backward induction procedure is initiated by adopting the terminal condition as specified in Eq. (3.6b).
- (ii) Time-stepping calculations between two consecutive monitoring dates
The relevant numerical schemes are derived based on the jump condition (3.6a), numerical quadrature rule (3.7) and CONV algorithm (3.11). All these are combined to effect numerical valuation of the two-dimensional expectation integral. For $k = N - 1, N - 2, \dots, 1$, the numerical approximation of $V(Z_{t_k}^-, \gamma_{t_k}, t_k^-)$ is given by

$$\begin{aligned}
&V(Z_{t_k}^-, \gamma_{t_k}, t_k^-) \\
&\approx \frac{e^{-r\Delta}}{2\pi} \sum_{j=1}^J w_j p_\gamma(\zeta_j | \gamma_{t_k}) \left[\mathbf{1}_{\{l < Z_{t_k}^- \leq b\}} \int_{-\infty}^{\infty} e^{-wZ_{t_k}^-} \hat{V}_\alpha(\beta, \zeta_j, t_{k+1}^-) \Psi(-w; \zeta_j, \gamma_{t_k}) d\beta \right. \\
&\quad \left. + \mathbf{1}_{\{Z_{t_k}^- > b\}} \int_{-\infty}^{\infty} e^{-wb} \hat{V}_\alpha(\beta, \zeta_j, t_{k+1}^-) \Psi(-w; \zeta_j, \gamma_{t_k}) d\beta \right].
\end{aligned} \tag{3.12a}$$

Since $Z_{t_0} \in (l, b]$ is assumed, the numerical approximation scheme for $k = 0$ is reduced to

$$V(Z_{t_0}, \gamma_{t_0}, t_0) \approx \frac{e^{-r\Delta}}{2\pi} \sum_{j=1}^J w_j p_\gamma(\zeta_j | \gamma_{t_0}) \int_{-\infty}^{\infty} e^{-wZ_{t_0}} \hat{V}_\alpha(\beta, \zeta_j, t_1^-) \Psi(-w; \zeta_j, \gamma_{t_0}) d\beta. \tag{3.12b}$$

The evaluation of the above Fourier integrals can be performed using the fast Fourier transform (FFT) method. In the usual FFT procedure, checking of the knock-out condition and dividend-barrier payout has to be revealed in the real domain, one has to perform inverse Fourier transform at each time step in the backward induction to recover the value function

in the real domain. In this paper, we adopt the use of the fast Hilbert transform method that can avoid the nuisance of recovering the value function at each of the monitoring instants. As explained below, such computational convenience is feasible since the barrier conditions are naturally incorporated in the fast Hilbert transform procedure.

Construction of the fast Hilbert transform algorithm

The key ingredient in the fast Hilbert transform method is that multiplying a function by the indicator function associated with the barrier feature in the real domain corresponds to taking Hilbert transform in the Fourier domain. As a result, instead of computing $N - 1$ steps of Fourier transform inversion and $N - 1$ steps of Fourier transform as shown in Eq. (3.12a), the fast Hilbert transform method only requires $N - 1$ steps of convolution computation with regard to the presence of the lower absorbing (ruined) barrier and upper reflecting (dividend) barrier.

The backward induction procedure in the Fourier domain using the fast Hilbert transform algorithm can be formulated as follows:

- (i) For $k = N$, we have the same terminal condition as specified in Eq. (3.6b). We take the generalized Fourier transform of the terminal payoff to obtain $\hat{V}_\alpha(\beta, \zeta_j, t_N^-)$ [see Eq. (3.19a)], where we set $\gamma_{t_N} = \zeta_j$, $j = 1, 2, \dots, N$.
- (ii) For the intermediate time steps, $k = N - 1, N - 2, \dots, 1$, the numerical approximation is given by

$$\begin{aligned} \hat{V}_\alpha(\beta, \zeta_p, t_k^-) \approx & e^{-r\Delta} \int_{-\infty}^{\infty} \sum_{j=1}^J w_j \hat{V}_\alpha(\eta, \zeta_j, t_{k+1}^-) \tilde{\Psi}(-\alpha - i\eta; \zeta_j, \zeta_p) e^{i\frac{(\beta-\eta)(t+b)}{2}} \frac{\sin \frac{(\beta-\eta)(b-l)}{2}}{\pi(\beta-\eta)} d\eta \\ & - \frac{e^{-r\Delta} e^{i\beta b}}{2\pi(\alpha + i\beta)} \sum_{j=1}^J w_j \int_{-\infty}^{\infty} e^{-i\eta b} \hat{V}_\alpha(\eta, \zeta_j, t_{k+1}^-) \tilde{\Psi}(-\alpha - i\eta; \zeta_j, \zeta_p) d\eta, \end{aligned} \quad (3.13a)$$

for $p = 1, 2, \dots, J$. Here, we set $\gamma_{t_{k+1}} = \zeta_j$ and $\gamma_{t_k} = \zeta_p$ in the conditional moment generating function $\Psi(w; \gamma_{t_{k+1}}, \gamma_{t_k})$, and write $\tilde{\Psi}(w; \zeta_j, \zeta_p)$ as $\Psi(w; \zeta_j, \zeta_p) p_\gamma(\zeta_j | \zeta_p)$.

- (iii) For the last step where $k = 0$, the numerical approximation to the value function at t_0 is obtained by

$$V(Z_{t_0}, \zeta_p, t_0) \approx \frac{e^{-r\Delta}}{2\pi} \sum_{j=1}^J w_j \int_{-\infty}^{\infty} e^{-(\alpha+i\beta)Z_{t_0}} \hat{V}_\alpha(\beta, \zeta_j, t_1^-) \tilde{\Psi}(-\alpha - i\beta; \zeta_j, \zeta_p) d\beta. \quad (3.13b)$$

To show how to derive the above fast Hilbert transform algorithm from Eqs. (3.6a) and (3.6b), we take the generalized Fourier transform on both sides of Eq. (3.12a), incorporating the indicator functions that model the ruined and dividend strategy features. Firstly, it is necessary to multiply the exponential damping factor $e^{\alpha Z_{t_k}^-}$ on both sides of Eq. (3.12a) in order that the Fourier transforms are well defined. Since both the inverse Fourier transform representation and the indicator function $\mathbf{1}_{\{l < Z_{t_k}^- \leq b\}}$ include the state variable $Z_{t_k}^-$ for the first term on the right hand side, we make use of the Hilbert transform formula (2.14b) to deal with the Fourier transform of the product of a function and an indicator function. Due to nonexistence of the state variable $Z_{t_k}^-$ in the inverse Fourier transform representation of the second term, we take the usual Fourier transform of the second term. In the next step, using a quadrature rule in the log-activity rate dimension, we perform the computation on a set of log-activity rate nodes, where $\gamma_{t_{k+1}} = \zeta_j$, $j = 1, 2, \dots, N$. The same set of log-activity

rate nodes are employed over all time points, which leads to Eq. (3.13a). In the last step, we compute $V(Z_{t_0}, \zeta_p, t_0)$ through one step inverse Fourier transform as shown in Eq. (3.13b).

The kernel function $\tilde{\Psi}(w; \zeta_j, \zeta_p)$ is the input that characterizes the time-changed Lévy processes. By combining Eqs. (A.2), (A.3) and (3.10), the Bessel function presented in $p_\gamma(\zeta_j|\zeta_p)$ cancels with the Bessel function in the denominator of $\Psi(w; \zeta_j, \zeta_p)$, leaving only one Bessel term. Furthermore, some special attention should be given to the calculation of $\tilde{\Psi}(w; \zeta_j, \zeta_p)$. First of all, it involves a modified Bessel function of the first kind, which increases dramatically in value when $q \rightarrow -1$ or $w \rightarrow \infty$. For computational convenience, the scaled Bessel function should be used instead. Secondly, some terms in $\tilde{\Psi}(w; \zeta_j, \zeta_p)$ may become quite large when certain set of parameters are chosen, so we have to simplify these multiplications in computing the numerical value for $\tilde{\Psi}(w; \zeta_j, \zeta_p)$. Lastly, one can either use a spline interpolation to obtain the value of $V(Z_{t_0}, \gamma_{t_0}, t_0)$ from $V(Z_{t_0}, \zeta_p, t_0)$, or choose the layout of the grid such that γ_{t_0} lies exactly on the grid.

Discrete approximation

We consider the inverse Fourier transform of g

$$Pg(x) = \frac{1}{2\pi} \int_{-\infty}^{\infty} e^{-i\beta x} g(\beta, \zeta_j) \tilde{\Psi}(-\alpha - i\beta; \zeta_j, \zeta_p) d\beta, \quad (3.14)$$

and evaluate the convolution integral in the following form

$$Qg(\beta) = \int_{-\infty}^{\infty} g(\eta, \zeta_j) \tilde{\Psi}(-\alpha - i\eta; \zeta_j, \zeta_p) e^{i\frac{(\beta-\eta)(l+b)}{2}} \frac{\sin \frac{(\beta-\eta)(b-l)}{2}}{\pi(\beta-\eta)} d\eta. \quad (3.15)$$

The inverse Fourier transform can be evaluated numerically by

$$P_{h,M}g(x) = \frac{1}{2\pi} \sum_{m=-M}^M e^{-ixmh} g(mh, \zeta_j) \tilde{\Psi}(-\alpha - imh; \zeta_j, \zeta_p) h, \quad (3.16)$$

while the numerical evaluation of $Qg(\beta)$ can be effected by the following discretized scheme at $\beta = nh$, where

$$Q_{h,M}g(nh) = \sum_{m=-M}^M g(mh, \zeta_j) \tilde{\Psi}(-\alpha - imh; \zeta_j, \zeta_p) e^{i\frac{h(n-m)(l+b)}{2}} \frac{\sin \frac{h(n-m)(b-l)}{2}}{\pi h(n-m)} h. \quad (3.17)$$

Here, $n = -M, \dots, M$, and h is the step size. The infinite domain is truncated to the finite truncation domain $[-Mh, Mh]$, where M is referred as the truncation level. The simple trapezoidal sum approximation is seen to achieve sufficiently high level of accuracy with exponentially decaying discretization errors.

Toeplitz matrix-vector multiplication

A matrix T is said to be a Toeplitz matrix or diagonal-constant matrix if $T_{n,m} = T_{n+1,m+1}$, where $T_{n,m}$ denotes the $(n, m)^{th}$ entry of T . The above convolution integral computation can be expressed as a Toeplitz matrix-vector multiplication. In our context, we define the corresponding Toeplitz matrix T whose entries are given by

$$T_{n,m} = \begin{cases} \frac{\sin \frac{h(n-m) \ln \frac{B}{L}}{2}}{\pi(n-m)} & m \neq n \\ \frac{h \ln \frac{B}{L}}{2\pi} & m = n \end{cases}. \quad (3.18)$$

The computation of the Toeplitz matrix-vector multiplication can be easily embedded into a circulant matrix. While the usual direct computational cost of the matrix-vector multiplication is $O(M^2)$, it is well known that the multiplication of a circulant matrix by a

vector can be implemented using the fast Fourier transform with computational complexity of $O(M \log_2 M)$.

Implementation procedures

We present the detailed implementation procedure of the fast Hilbert transform algorithm for computing the firm asset value function where the firm asset value process is modeled as a time-changed Lévy process with an upper reflecting barrier and a lower absorbing barrier. Firstly, it is necessary to choose a proper factor α to guarantee the existence of the generalized Fourier transforms. Note that $V(Z_{t_N^-}, \gamma_{t_N}, t_N^-) = e^{Z_{t_N^-}} \mathbf{1}_{\{l < Z_{t_N^-} \leq b\}} + B \mathbf{1}_{\{Z_{t_N^-} > b\}} \in L^1(\mathbb{R})$ for any $\alpha < 0$. Also, recall that $\alpha \in \mathcal{L}_X$, so we have $\alpha \in (\lambda_-, 0)$.

Step 1: Preparation

Calculate the generalized Fourier transform of the terminal payoff using the analytic formula

$$\hat{V}_\alpha(\beta, \zeta_j, t_N^-) = \frac{B e^{(\alpha+i\beta)b} - L e^{(\alpha+i\beta)l}}{\alpha + i\beta + 1} - \frac{B e^{(\alpha+i\beta)b}}{\alpha + i\beta}, \quad \beta = -Mh, \dots, Mh. \quad (3.19a)$$

Prepare the matrix with elements $\tilde{\Psi}(-\alpha - imh; \zeta_j, \zeta_p)$ for $p = 1, 2, \dots, J$.

Step 2: Backward induction in the Fourier domain

Based on Eqs. (3.13a) and (3.17), by interchanging the order of summations, we compute $\hat{V}_\alpha(\beta, \zeta_p, t_k^-)$ as follows

$$\begin{aligned} & \hat{V}_\alpha(\beta, \zeta_p, t_k^-) \\ & \approx e^{-r\Delta} e^{i\frac{\beta(l+b)}{2}} \sum_{m=-M}^M e^{-i\frac{mh(l+b)}{2}} \sum_{j=1}^J w_j \hat{V}_\alpha(mh, \zeta_j, t_{k+1}^-) \tilde{\Psi}(-\alpha - imh; \zeta_j, \zeta_p) \frac{\sin \frac{(\beta-mh)(b-l)}{2}}{\pi(\beta - mh)} h \\ & - \frac{e^{-r\Delta} e^{i\beta b}}{2\pi(\alpha + i\beta)} \sum_{m=-M}^M e^{-imhb} \sum_{j=1}^J w_j \hat{V}_\alpha(mh, \zeta_j, t_{k+1}^-) \tilde{\Psi}(-\alpha - imh; \zeta_j, \zeta_p) h, \end{aligned} \quad (3.19b)$$

where $\beta = -Mh, \dots, Mh$.

Repeat Step 2 for $k = N - 1, \dots, 1$.

Step 3: Inversion of Fourier transform at the final step to recover the value function

We approximate the inverse Fourier transform representation in Eq. (3.13b) by a numerical quadrature rule to recover the value function at time t_0 as follows

$$V(Z_{t_0}, \zeta_p, t_0) \approx \frac{e^{-r\Delta}}{2\pi} \sum_{j=1}^J w_j \sum_{m=-M}^M e^{-(\alpha+imh)Z_{t_0}} \hat{V}_\alpha(mh, \zeta_j, t_1^-) \tilde{\Psi}(-\alpha - imh; \zeta_j, \zeta_p) h. \quad (3.19c)$$

One can use a spline interpolation to obtain $V(Z_{t_0}, \gamma_{t_0}, t_0)$ from the grid value functions $V(Z_{t_0}, \zeta_p, t_0)$, $p = 1, 2, \dots, J$.

Remarks

1. Since the initial firm asset value A_0 is substituted into the pricing formulation only in the final step of the algorithm, the fast Hilbert transform algorithm can be used to find the value function at varying values of A_0 simultaneously with almost no additional computational cost.

2. Like other Fourier option pricing algorithms, the fast Hilbert transform algorithm can compute the delta and gamma of the value function with essentially no additional computational effort.

We write $\hat{V}_\alpha(nh, \zeta_p, t_k)$ as the grid function for $\hat{V}_\alpha(\beta, \zeta_p, t_k^-)$ at $\beta = nh$. To deal with the lower absorbing (ruined) barrier and upper reflecting (dividend) barrier, we replace the backward induction procedure in Eq. (3.19b) by

$$\begin{aligned} & \hat{V}_\alpha(nh, \zeta_p, t_k) \\ = & e^{-r\Delta} \left\{ e^{i\frac{nh(l+b)}{2}} \sum_{m=-M, m \neq n}^M e^{-i\frac{mh(l+b)}{2}} \sum_{j=1}^J w_j \hat{V}_\alpha(mh, \zeta_j, t_{k+1}) \tilde{\Psi}(-\alpha - imh; \zeta_j, \zeta_p) \frac{\sin \frac{h(n-m) \ln \frac{B}{L}}{2}}{\pi(n-m)} \right. \\ & \left. + \sum_{j=1}^J w_j \hat{V}_\alpha(nh, \zeta_j, t_{k+1}) \tilde{\Psi}(-\alpha - inh; \zeta_j, \zeta_p) \frac{h \ln \frac{B}{L}}{2\pi} \right\} \\ & - \frac{e^{-r\Delta} e^{inhb}}{2\pi(\alpha + inh)} \sum_{m=-M}^M e^{-imhb} \sum_{j=1}^J w_j \hat{V}_\alpha(mh, \zeta_j, t_{k+1}) \tilde{\Psi}(-\alpha - imh; \zeta_j, \zeta_p) h, \quad (3.20) \end{aligned}$$

where $n = -M, \dots, M$. Since the above computation involves a Toeplitz matrix-vector multiplication at each time step, the backward induction in the Fourier domain can be formulated in an easier readable format in matrix/vector notation in Step 2. We introduce the following notations: $\hat{V}_\alpha(t_{k+1})$ is a $(2M+1) \times J$ matrix with elements $\hat{V}_\alpha(mh, \zeta_j, t_{k+1})$, $\tilde{\Psi}(\zeta_p)$ is a $(2M+1) \times J$ matrix with elements $\tilde{\Psi}(-\alpha - imh; \zeta_j, \zeta_p)$ for $p = 1, 2, \dots, J$, \mathbf{w} is a column vector containing the quadrature weights. We construct the following matrix/vector multiplication

$$\boldsymbol{\kappa}_p(t_k) = [\hat{V}_\alpha(t_{k+1}) \cdot \tilde{\Psi}(\zeta_p)] \mathbf{w}, \quad p = 1, 2, \dots, J;$$

$$B(t_k) = [\boldsymbol{\kappa}_1(t_k), \boldsymbol{\kappa}_2(t_k), \dots, \boldsymbol{\kappa}_J(t_k)],$$

where $\boldsymbol{\kappa}_p(t_k)$ is a column vector of dimension $2M+1$, $B(t_k)$ is a $(2M+1) \times J$ matrix, and the operator “ \cdot ” denotes an element-wise matrix-matrix product.

Let H and F be the $(2M+1) \times J$ matrices whose entries are $H_{m,p} = e^{-i\frac{mh(b+l)}{2}}$ and $F_{m,p} = e^{i\frac{mh(b+l)}{2}}$, respectively. Also, let $\boldsymbol{\xi}$ and \mathbf{s} be the column vectors composed of elements from $\boldsymbol{\xi}_m = e^{-imhb}h$ and $\mathbf{s}_m = \frac{e^{imhb}}{\alpha + imh}$, respectively. According to Eq. (3.20), we can rewrite the backward induction in the Fourier domain in the following matrix/vector form

$$\hat{V}_\alpha(t_k) = e^{-r\Delta} [T(B(t_k) \cdot H)] \cdot F - \frac{e^{-r\Delta}}{2\pi} \mathbf{s} [\boldsymbol{\xi}^T B(t_k)], \quad (3.21)$$

where T is the Toeplitz matrix defined in Eq. (3.18). We take advantage of the matrix-vector multiplication in the Toeplitz matrix, which can achieve $O(M \log_2 M)$ complexity in the log-asset return dimension. Moreover, the same Toeplitz matrix is used from step to step. Only two runs of the fast Fourier transform are required for each time step. In fact, we only need to update $B(t_k)$ to recover $\hat{V}_\alpha(t_k)$ at each time step.

The enhanced version of the fast Hilbert transform algorithm is summarized in the table below.

Algorithm: Pricing dividend-ruin firm asset value model under time-changed Lévy processes.

Preparation

- Calculate $\widehat{V}_\alpha(t_N)$ using the analytic formula (3.19a);
- Prepare matrix $\widetilde{\Psi}(\zeta_p)$ for $p = 1, 2, \dots, J$;
- Prepare matrices H, F , and vectors $\boldsymbol{\xi}, \mathbf{s}$;
- Calculate the first row and column of the Toeplitz matrix T .

Backward induction

- Calculate $\boldsymbol{\kappa}_p(t_k) = [\widehat{V}_\alpha(t_{k+1}) \cdot \widetilde{\Psi}(\zeta_p)] \mathbf{w}$ for $p = 1, 2, \dots, J$, and update $B(t_k)$;
- Compute $\widehat{V}_\alpha(t_k)$ by Eq. (3.21) using FFT algorithm for $k = N - 1, \dots, 1$.

Firm asset value function at t_0

- Calculate the firm asset value function by Eq. (3.19c). Use a spline interpolation to obtain $V(Z_{t_0}, \gamma_{t_0}, t_0)$.

Computational complexity

We adopt the Gauss-Legendre quadrature rule in the log-activity rate dimension. The computational effort in the preparation step with non-equidistant quadrature rules is dominated by the computation of the matrices $\widetilde{\Psi}(\zeta_p)$, $p = 1, 2, \dots, J$, which involve numerical valuation of the modified Bessel functions. Recall that the computation of the modified Bessel function costs significantly more than a simple multiplication. More precisely, suppose the computation of the Bessel function costs \mathcal{A} times the number of operations needed for a multiplication, the matrices $\widetilde{\Psi}(\zeta_p)$, $p = 1, 2, \dots, J$ would require $O(\mathcal{A}MJ^2)$ operations to compute all matrix elements.

As far as the computation in the main loop of the algorithm is concerned, it is dominated by the term $[T(B(t_k) \cdot H)] \cdot F$. Since the computation of the vector $\boldsymbol{\kappa}_p(t_k)$ costs $O(MJ)$ operations, it leads to $O(MJ^2)$ complexity for the calculation of the matrix $B(t_k)$. The computation of the product $\mathbf{s}[\boldsymbol{\xi}^T B(t_k)]$ costs $O(MJ^2)$ operations. The overall computational complexity for the term $[T(B(t_k) \cdot H)] \cdot I$ is $O(M \log_2 MJ^2)$ by taking advantage of the special structure of the Toeplitz matrix T and the use of fast Fourier transform. The complexity is lower compared to a direct computation with computational complexity $O(M^2J^2)$. As a result, the overall complexity of the fast Hilbert transform algorithm is $O(\max[\mathcal{A}, N \log_2 M]MJ^2)$.

In summary, the essence of the fast Hilbert transform method is that the numerical computation remains in the Fourier domain and only one Fourier inversion is required in the final step. The fast Fourier transform method requires twice as many computations as the Hilbert transform method. This is because we need to compute both the Fourier transform and the inverse Fourier transform at each monitoring time instant in the backward induction. Also, it is well known that the FFT method has to observe a restriction on the step size, where $\Delta_x \Delta_\beta = 2\pi/M$. Furthermore, the trapezoidal quadrature rule used in computing the Fourier transform of option value is second order accurate in the discretization step size in the dimension of log-asset return. Feng and Linetsky (2008) show that if one adopts the fast Hilbert transform method, the trapezoidal quadrature rule used in computing the inverse Fourier transform (3.14) and convolution integral (3.15) has exponentially decaying errors due to analyticity of the integrand in the appropriate strip in the complex plane.

4 Bermudan options

In this section, we would like to discuss the fast Hilbert transform algorithm for pricing Bermudan options under time-changed Lévy processes, where the computational procedures involve numerical evaluation of a sequence of inverse Fourier and Hilbert transforms. Our pricing algorithm is developed by applying the fast Hilbert transform method in the log-asset return dimension and adopting the quadrature rule in the numerical integration of the log-activity rate of stochastic time change. Suppose the current time is $t_0 = 0$ and the set of monitoring times for the Bermudan option is denoted by $\mathcal{T} = \{t_1, \dots, t_N\}$, where $t_N = T$ is maturity. By assuming a uniform time interval Δ , we set $t_k = k\Delta$, $k = 0, 1, \dots, N$. The Bermudan option can be exercised at any time $t_k \in \mathcal{T}$ with the exercise payoff $\tilde{G}(S_{t_k})$. Note that $\tilde{G}(S) = (S - K)^+$ for the call payoff and $\tilde{G}(S) = (K - S)^+$ for the put payoff, where K is the strike price. In this paper, we focus our discussion on pricing Bermudan put options and similar pricing approach can be applied to Bermudan call options. Also, pricing of an American option can be achieved by taking the limit of vanishing time interval between successive monitoring dates in the Bermudan option counterpart; that is, taking $\Delta \rightarrow 0$.

Determination of the critical asset prices

The optimal stopping problem of a Bermudan put option is characterized by the set of critical asset prices to be determined at all monitoring times below which it is optimal for the option holder to exercise the Bermudan put option. The main step in the fast Hilbert transform algorithm is the determination of the critical asset price $S_k^*(\gamma_{t_k})$ at monitoring time t_k and level γ_{t_k} of the log-activity rate under time-changed Lévy processes, $k = 1, 2, \dots, N$. Assuming the underlying asset to be non-dividend paying, it is known that the critical asset price $S_N^*(\gamma_{t_N})$ is K at maturity t_N . The critical asset prices $S_k^*(\gamma_{t_k})$, $k = N - 1, N - 2, \dots, 1$ are determined successively using backward induction. First of all, we would like to establish the existence of a unique value for $S_k^*(\gamma_{t_k})$ where $0 < S_k^*(\gamma_{t_k}) < K$ for $k = N - 1, N - 2, \dots, 1$.

Proposition 1 *Assuming $r \geq 0$, for $k = 1, 2, \dots, N - 1$, there exists a unique critical asset price $S_k^*(\gamma_{t_k})$ where $0 < S_k^*(\gamma_{t_k}) < K$ such that the Bermudan put option value $\tilde{V}(S_{t_k}, \gamma_{t_k}, t_k)$ satisfies*

$$\tilde{V}(S_{t_k}, \gamma_{t_k}, t_k) = \tilde{G}(S_{t_k})\mathbf{1}_{(0, S_k^*(\gamma_{t_k})]} + e^{-r\Delta} E_{t_k}[\tilde{V}(S_{t_{k+1}}, \gamma_{t_{k+1}}, t_{k+1})]\mathbf{1}_{(S_k^*(\gamma_{t_k}), \infty)}, \quad (4.1)$$

where E_{t_k} denotes the expectation conditional on S_{t_k} and γ_{t_k} .

The proof of Proposition 1 is relegated to Appendix B. At the monitoring instant t_k , for any given level γ_{t_k} of the log-activity rate, it is optimal to exercise the Bermudan put option when S_{t_k} lies in the exercise region $(0, S_k^*(\gamma_{t_k})]$ and the option remains alive when S_{t_k} lies in the continuation region $(S_k^*(\gamma_{t_k}), \infty)$. The exercise region and continuation region are separated by the critical asset price $S_k^*(\gamma_{t_k})$. The continuation value $\tilde{C}(S_{t_k}, \gamma_{t_k}, t_k)$ is given by $e^{-r\Delta} E_{t_k}[\tilde{V}(S_{t_{k+1}}, \gamma_{t_{k+1}}, t_{k+1})]$.

Backward induction in the state space

We consider the log-asset return process normalized by the strike price K under the time-changed Lévy process X_{T_t} as follows

$$Y_t = \ln \frac{S_t}{K} = rt + X_{T_t}. \quad (4.2)$$

For a Bermudan put option, the exercise payoff at a monitoring date t_k is given by $G(Y_{t_k}) = \tilde{G}(S_{t_k}) = K(1 - e^{Y_{t_k}})^+$. We write the Bermudan put option value and continuation value as

$V(Y_t, \gamma_t, t) = \tilde{V}(S_t, \gamma_t, t)$ and $C(Y_t, \gamma_t, t) = \tilde{C}(S_t, \gamma_t, t)$, respectively. At any monitoring time, the price of the Bermudan put option is given by the maximum of the continuation value and exercise payoff. Given N discrete monitoring dates, where $\mathcal{T} = \{t_k | k = 1, \dots, N\}$ with $t_N = T$, the Bermudan put option pricing formula can be expressed as

$$V(Y_{t_k}, \gamma_{t_k}, t_k) = \begin{cases} G(Y_{t_N}) & \text{for } k = N \\ \max\{C(Y_{t_k}, \gamma_{t_k}, t_k), G(Y_{t_k})\} & \text{for } k = 1, 2, \dots, N-1. \\ C(Y_{t_0}, \gamma_{t_0}, t_0) & \text{for } k = 0 \end{cases}$$

Continuation value

We express the continuation value $C(Y_{t_k}, \gamma_{t_k}, t_k)$ as a two-dimensional expectation integral and evaluate the expectation in the log-activity rate dimension using numerical integration. Using the tower property and an appropriate quadrature rule, the continuation value at the monitoring time t_k is given by

$$\begin{aligned} C(Y_{t_k}, \gamma_{t_k}, t_k) &= e^{-r\Delta} E[E[V(Y_{t_{k+1}}, \gamma_{t_{k+1}}, t_{k+1}) | \mathcal{F}_{t_k}, \gamma_{t_{k+1}}] | \mathcal{F}_{t_k}] \\ &\approx e^{-r\Delta} \sum_{j=1}^J w_j p_\gamma(\zeta_j | \gamma_{t_k}) E[V(Y_{t_{k+1}}, \gamma_{t_{k+1}}, t_{k+1}) | \mathcal{F}_{t_k}, \gamma_{t_{k+1}} = \zeta_j]. \end{aligned} \quad (4.3)$$

where ζ_j , $j = 1, 2, \dots, J$ are the node points in the quadrature rule for the log-activity rate. Next, the inner expectation is evaluated numerically in the Fourier domain via the CONV method. Applying the usual procedure of damping the value functions, we define $C_\alpha(Y_t, \gamma_t, t) = e^{\alpha Y_t} C(Y_t, \gamma_t, t)$, $V_\alpha(Y_t, \gamma_t, t) = e^{\alpha Y_t} V(Y_t, \gamma_t, t)$ and $G_\alpha(Y_t) = e^{\alpha Y_t} G(Y_t)$. By following a similar procedure that derives the inner expectation integral in terms of inverse Fourier transform representation, we obtain

$$E[V(Y_{t_{k+1}}, \gamma_{t_{k+1}}, t_{k+1}) | \mathcal{F}_{t_k}, \gamma_{t_{k+1}} = \zeta_j] = \frac{1}{2\pi} \int_{-\infty}^{\infty} e^{-w Y_{t_k}} \hat{V}_\alpha(\beta, \zeta_j, t_{k+1}) \Psi(-w; \zeta_j, \gamma_{t_k}) d\beta, \quad (4.4)$$

where $w = \alpha + i\beta$ and $\hat{V}_\alpha(\beta, \gamma_t, t)$ denotes the generalized Fourier transform of $V(Y_t, \gamma_t, t)$. The combination of Eqs. (4.3) and (4.4) leads to the following analytic approximation formula

$$C_\alpha(Y_{t_k}, \gamma_{t_k}, t_k) \approx \frac{e^{-r\Delta}}{2\pi} \sum_{j=1}^J w_j \int_{-\infty}^{\infty} e^{-i\beta Y_{t_k}} \hat{V}_\alpha(\beta, \zeta_j, t_{k+1}) \tilde{\Psi}(-w; \zeta_j, \gamma_{t_k}) d\beta, \quad (4.5)$$

where $\tilde{\Psi}(w; \zeta_j, \gamma_{t_k}) = \Psi(w; \zeta_j, \gamma_{t_k}) p_\gamma(\zeta_j | \gamma_{t_k})$.

Fourier transform algorithm

Given N discrete monitoring dates as characterized by the point set $\mathcal{T} = \{t_k | k = 1, \dots, N\}$ with $t_N = T$, the backward induction procedure for pricing a Bermudan put option can be summarized as follows:

1. Initiation of the (damped) value function as specified by the terminal payoff

$$V_\alpha(Y_{t_N}, \gamma_{t_N}, t_N) = G_\alpha(Y_{t_N}). \quad (4.6a)$$

2. Determination of the critical asset prices and backward induction calculations of the option value

We let $x_k^*(\gamma_{t_k}) = \ln S_k^*(\gamma_{t_k})$. At the critical asset price $x_k^*(\gamma_{t_k})$, we have equality of the

exercise payoff and continuation value. For $k = N - 1, N - 2, \dots, 1$, $x_k^*(\gamma_{t_k})$ solves the algebraic equation

$$G_\alpha(x) = \frac{e^{-r\Delta}}{2\pi} \sum_{j=1}^J w_j \int_{-\infty}^{\infty} e^{-i\beta x} \hat{V}_\alpha(\beta, \zeta_j, t_{k+1}) \tilde{\Psi}(-\alpha - i\beta; \zeta_j, \gamma_{t_k}) d\beta. \quad (4.6b)$$

The (damped) option value at time t_k is approximated by

$$\begin{aligned} & V_\alpha(Y_{t_k}, \gamma_{t_k}, t_k) \\ & \approx \mathbf{1}_{(-\infty, x_k^*(\gamma_{t_k})]} G_\alpha(Y_{t_k}) \\ & + \mathbf{1}_{(x_k^*(\gamma_{t_k}), \infty)} \frac{e^{-r\Delta}}{2\pi} \sum_{j=1}^J w_j \int_{-\infty}^{\infty} e^{-i\beta Y_{t_k}} \hat{V}_\alpha(\beta, \zeta_j, t_{k+1}) \tilde{\Psi}(-\alpha - i\beta; \zeta_j, \gamma_{t_k}) d\beta. \end{aligned} \quad (4.6c)$$

The above procedure illustrates the implementation of the backward induction using the Fourier transform based method, where $N - 1$ steps of Fourier transform inversion and $N - 1$ steps of Fourier transform are performed. However, we would like to reformulate the backward induction calculations by taking advantage of the elegant properties of the fast Hilbert transform method.

The fast Hilbert transform algorithm for Bermudan put options

The backward induction in the Fourier domain can proceed as follows. We start with $k = N$, where

$$\hat{V}_\alpha(\beta, \zeta_j, t_N) = \hat{G}_\alpha(\beta), \quad j = 1, 2, \dots, J. \quad (4.7a)$$

For $k = N - 1, N - 2, \dots, 1$, we apply an efficient root-finding method (like the Newton-Raphson method) to find $x_{k,p}^*$ by solving Eq. (4.6b) on each log-activity rate node $\gamma_{t_k} = \zeta_p$, $p = 1, 2, \dots, J$. The numerical approximation of $\hat{V}_\alpha(\beta, \zeta_p, t_k)$ is given in terms of the Hilbert transform

$$\begin{aligned} \hat{V}_\alpha(\beta, \zeta_p, t_k) & \approx \mathcal{F}(G_\alpha(Y_{t_k}) \mathbf{1}_{(-\infty, x_{k,p}^*]})(\beta) \\ & + \frac{e^{-r\Delta}}{2} \sum_{j=1}^J w_j \hat{V}_\alpha(\beta, \zeta_j, t_{k+1}) \tilde{\Psi}(-\alpha - i\beta; \zeta_j, \zeta_p) \\ & + \frac{ie^{-r\Delta}}{2} e^{i\beta x_{k,p}^*} \mathcal{H}\left(e^{-i\eta x_{k,p}^*} \sum_{j=1}^J w_j \hat{V}_\alpha(\eta, \zeta_j, t_{k+1}) \tilde{\Psi}(-\alpha - i\eta; \zeta_j, \zeta_p)\right)(\beta), \end{aligned} \quad (4.7b)$$

for $p = 1, 2, \dots, J$. The numerical approximation to the Bermudan put option value at initiation is given by

$$V(Y_{t_0}, \zeta_p, t_0) \approx \frac{e^{-r\Delta}}{2\pi} \sum_{j=1}^J w_j \int_{-\infty}^{\infty} e^{-(\alpha+i\beta)Y_{t_0}} \hat{V}_\alpha(\beta, \zeta_j, t_1) \tilde{\Psi}(-\alpha - i\beta; \zeta_j, \zeta_p) d\beta. \quad (4.7c)$$

The justification of the above backward induction procedure is presented below. Firstly, we need to determine the critical asset prices. By setting $\gamma_{t_k} = \zeta_p$, $p = 1, 2, \dots, J$, we use Eq. (4.6b) to obtain the critical asset prices. Note that the Fourier transform of $\int_{-\infty}^{\infty} e^{-i\beta Y_{t_k}} \hat{V}_\alpha(\beta, \zeta_j, t_{k+1}) \tilde{\Psi}(-\alpha - i\beta; \zeta_j, \gamma_{t_k}) d\beta$ is the product $\hat{V}_\alpha(\beta, \zeta_j, t_{k+1}) \tilde{\Psi}(-\alpha - i\beta; \zeta_j, \gamma_{t_k})$. Taking the Fourier transform on both sides of Eq. (4.6c) and using the Hilbert transform

formula Eq. (2.14a), we obtain

$$\begin{aligned}\hat{V}_\alpha(\beta, \gamma_{t_k}, t_k) &\approx \mathcal{F}(G_\alpha(Y_{t_k})\mathbf{1}_{(-\infty, x_k^*(\gamma_{t_k})]})(\beta) \\ &+ \frac{e^{-r\Delta}}{2} \sum_{j=1}^J w_j \hat{V}_\alpha(\beta, \zeta_j, t_{k+1}) \tilde{\Psi}(-\alpha - i\beta; \zeta_j, \gamma_{t_k}) \\ &+ \frac{ie^{-r\Delta}}{2} e^{i\beta x_k^*(\gamma_{t_k})} \mathcal{H}\left(e^{-i\eta x_k^*(\gamma_{t_k})} \sum_{j=1}^J w_j \hat{V}_\alpha(\eta, \zeta_j, t_{k+1}) \tilde{\Psi}(-\alpha - i\eta; \zeta_j, \gamma_{t_k})\right)(\beta).\end{aligned}$$

Setting $\gamma_{t_k} = \zeta_p$, $p = 1, 2, \dots, J$, we obtain Eq. (4.7b). Finally, since the inverse Fourier transform representation of $e^{-r\Delta}E[V(Y_{t_1}, \zeta_j, t_1)|\mathcal{F}_{t_0}]$ gives the continuation value at time t_0 [see Eq. (4.5)], we obtain the Bermudan put option value at initiation as shown in Eq. (4.7c).

Discrete approximation

In the fast Hilbert transform algorithm for pricing Bermudan options, we also need to evaluate the Hilbert transform of the following form

$$Rg(\beta) = \mathcal{H}\left(e^{-i\eta x}g(\eta, \zeta_j)\tilde{\Psi}(-\alpha - i\eta; \zeta_j, \zeta_p)\right)(\beta), \quad (4.8)$$

which can be evaluated by the truncated Sinc approximation [see Eq. (2.15)] as follows

$$R_{h,M}g(\beta) = \sum_{m=-M}^M e^{-imhx}g(mh, \zeta_j)\tilde{\Psi}(-\alpha - imh; \zeta_j, \zeta_p)\frac{1 - \cos\frac{\pi(\beta-mh)}{h}}{\frac{\pi(\beta-mh)}{h}}. \quad (4.9a)$$

Here, $\beta = -Mh, \dots, Mh$, h is the step size and M is the truncation level. The trapezoidal sum approximation is highly accurate, exhibiting exponentially decaying discretization errors. In this case, the corresponding Toeplitz matrix is given by

$$T_{n,m} = \frac{1 - \cos\frac{\pi(nh-mh)}{h}}{\frac{\pi(nh-mh)}{h}} = \begin{cases} \frac{1-(-1)^{n-m}}{\pi(n-m)} & m \neq n \\ 0 & m = n \end{cases}. \quad (4.9b)$$

Based on Eqs. (4.7b) and (4.9a), by substituting the elements of the Toeplitz matrix defined in Eq. (4.9b), we obtain

$$\begin{aligned}&\hat{V}_\alpha(nh, \zeta_p, t_k) \\ &= \mathcal{F}(G_\alpha(Y_{t_k}, t_k)\mathbf{1}_{(-\infty, x_{k,p}^*]})(nh) + \frac{e^{-r\Delta}}{2} \sum_{j=1}^J w_j \hat{V}_\alpha(nh, \zeta_j, t_{k+1}) \tilde{\Psi}(-\alpha - inh; \zeta_j, \zeta_p) \\ &+ \frac{ie^{-r\Delta}e^{inhx_{k,p}^*}}{2} \sum_{m=-M, m \neq n}^M e^{-imhx_{k,p}^*} \sum_{j=1}^J w_j \hat{V}_\alpha(mh, \zeta_j, t_{k+1}) \tilde{\Psi}(-\alpha - imh; \zeta_j, \zeta_p) \frac{1 - (-1)^{n-m}}{\pi(n-m)},\end{aligned} \quad (4.10)$$

where $n = -M, \dots, M$. Next, we approximate the initial option value using the trapezoidal rule as follows

$$V(Y_{t_0}, \zeta_p, t_0) \approx \frac{e^{-r\Delta}}{2\pi} \sum_{j=1}^J w_j \sum_{m=-M}^M e^{-(\alpha+imh)Y_{t_0}} \hat{V}_\alpha(mh, \zeta_j, t_1) \tilde{\Psi}(-\alpha - imh; \zeta_j, \zeta_p)h. \quad (4.11)$$

Similar to the dividend-ruin model, the backward induction calculations performed in the Fourier domain can be formulated in an easy readable format in matrix/vector notation. We construct the following matrix/vector multiplication:

$$\boldsymbol{\kappa}_p(t_k) = [\hat{V}_\alpha(t_{k+1}) \cdot \tilde{\Psi}(\zeta_p)]\mathbf{w}, \quad p = 1, 2, \dots, J;$$

$$B(t_k) = [\boldsymbol{\kappa}_1(t_k), \boldsymbol{\kappa}_2(t_k), \dots, \boldsymbol{\kappa}_J(t_k)],$$

where $\boldsymbol{\kappa}_p(t_k)$ is a column vector of dimension $2M + 1$, $B(t_k)$ is a $(2M + 1) \times J$ matrix, and the operator “ \cdot ” denotes an element-wise matrix-matrix product. Let H, F and \hat{G} be $(2M + 1) \times J$ matrices whose entries are $H_{m,p}(t_k) = e^{-imhx_{k,p}^*}$, $F_{m,p}(t_k) = e^{imhx_{k,p}^*}$ and $\hat{G}_{m,p}(t_k) = \mathcal{F}(G_\alpha(Y_{t_k}, t_k) \mathbf{1}_{(-\infty, x_{k,p}^*]})(mh)$, respectively. According to Eq. (4.10), we can rewrite the backward induction in the Fourier domain in the following matrix/vector form

$$\hat{V}_\alpha(t_k) = \hat{G}(t_k) + \frac{e^{-r\Delta}}{2} B(t_k) + \frac{e^{-r\Delta} i}{2} [T(B(t_k) \cdot H(t_k))] \cdot F(t_k). \quad (4.12)$$

Taking advantage of the structure of the Toeplitz matrix, the FFT algorithm can be applied to achieve $O(M \log_2 M)$ complexity in the dimension of the log-asset return.

Root-finding procedure for solving the critical asset prices

The fast Hilbert transform algorithm for pricing a Bermudan put option involves the determination of the critical asset prices. We adopt an efficient root-finding procedure, like the Newton-Raphson method to solve Eq. (4.6b) at varying values of γ_{t_k} that are set equal to ζ_p , $p = 1, 2, \dots, J$. An initial guess is needed when using the Newton-Raphson method. For example, we may start with the initial guess $x_{k,p}^* = x_{k+1,p}^*$ or $x_{k,p}^* = x_{k,p-1}^*$. Suppose $f(x) = 0$ is the equation whose root is to be found. Let the current iterate be \tilde{x} , the Newton-Raphson method determines the next iterate by replacing \tilde{x} by $\tilde{x} - f(\tilde{x})/f'(\tilde{x})$. In our context, we approximate the corresponding $f(x)$ and $f'(x)$ by using the trapezoidal rule with the step size h and truncation level M as follows

$$f(x) = \frac{e^{-r\Delta}}{2\pi} \sum_{j=1}^J w_j \sum_{m=-M}^M e^{-imhx} \hat{V}_\alpha(mh, \zeta_j, t_{k+1}) \tilde{\Psi}(-\alpha - imh; \zeta_j, \zeta_p) h - G_\alpha(x),$$

$$f'(x) = -\frac{e^{-r\Delta} i}{2\pi} \sum_{j=1}^J w_j \sum_{m=-M}^M e^{-imhx} mh \hat{V}_\alpha(mh, \zeta_j, t_{k+1}) \tilde{\Psi}(-\alpha - imh; \zeta_j, \zeta_p) h - G'_\alpha(x),$$

where $G'_\alpha(x) = Ke^{\alpha x}[\alpha - (1 + \alpha)e^x]$. The root-finding procedure is repeated until $|f(\tilde{x})/f'(\tilde{x})| < \varepsilon$, where ε is some small tolerance value.

Generalized Fourier transform of payoff conditional on early exercise

For a Bermudan put option, the (damped) exercise payoff is given by $G_\alpha(Y_{t_k}) = Ke^{\alpha Y_{t_k}}(1 - e^{Y_{t_k}})^+ \in L^1(R)$ for any $\alpha > 0$, $k = 1, 2, \dots, N$. Recall $\alpha \in \mathcal{L}_X$ and together with $\alpha > 0$, so we have $\alpha \in (0, \lambda_+)$. We calculate the generalized Fourier transform of the product of the exercise payoff and indicator function via the following Fourier transform formula

$$\mathcal{F}(G_\alpha(Y_{t_k}) \mathbf{1}_{(-\infty, x_{k,p}^*]})(\beta) = \begin{cases} \frac{K}{(\alpha + i\beta)(\alpha + i\beta + 1)} & k = N \\ K \left(\frac{1}{\alpha + i\beta} - \frac{e^{x_{k,p}^*}}{\alpha + i\beta + 1} \right) e^{(\alpha + i\beta)x_{k,p}^*} & k = N - 1, \dots, 1 \end{cases}, \quad (4.13)$$

where $\beta = -Mh, \dots, Mh$.

The enhanced version of the fast Hilbert transform algorithm is summarized in the table below.

Algorithm: Pricing Bermudan put options under time-changed Lévy processes.

Preparation

Calculate $\hat{V}_\alpha(t_N)$ using the Fourier transform (4.13) for $k = N$;
 Prepare the matrix $\tilde{\Psi}(\zeta_p)$ for $p = 1, 2, \dots, J$;
 Calculate the first row and column of the Toeplitz matrix T .

Backward induction

Determine the critical asset prices by the Newton-Raphson root-finding method;
 Update $H(t_k)$, $F(t_k)$ and $\hat{G}(t_k)$;
 Calculate $\kappa_p(t_k) = [\hat{V}_\alpha(t_{k+1}) \cdot \tilde{\Psi}(\zeta_p)]\mathbf{w}$ for $p = 1, 2, \dots, J$, and update $B(t_k)$;
 Compute $\hat{V}_\alpha(t_k)$ by Eq. (4.12) using FFT algorithm for $k = N - 1, \dots, 1$.

Initial option value

Calculate the initial option value by Eq. (4.11). Use a spline interpolation to obtain $V(Y_{t_0}, \gamma_{t_0}, t_0)$.

Computational complexity

We adopt the Gauss-Legendre quadrature rule in the log-activity rate dimension. The computational effort in the preparation step with non-equidistant quadrature rules is dominated by the computation of the matrices $\tilde{\Psi}(\zeta_p)$, $p = 1, 2, \dots, J$, which require $O(\mathcal{A}MJ^2)$ operations to compute all matrix elements.

We determine the critical asset prices by the Newton-Raphson method in the main loop of the algorithm. Numerical tests show that 3 to 4 iterations are sufficient to achieve accurate solution within good tolerance limit. The computational cost in the above step is $O(MJ^2)$. In fact, the computation in the main loop is dominated by numerical evaluation of the elements in $[T(B(t_k) \cdot H(t_k))] \cdot I(t_k)$. Since the calculation of the components in the vector $\kappa_p(t_k)$ costs $O(MJ)$ operations, it leads to $O(MJ^2)$ complexity for the calculation of the elements in the matrix $B(t_k)$. Hence, the overall computational complexity for $[T(B(t_k) \cdot H(t_k))] \cdot I(t_k)$ is $O(M \log_2 MJ^2)$, which is achieved by taking advantage of the special structure of the Toeplitz matrix T and the use of the fast Fourier transform. As a result, the overall complexity of the fast Hilbert transform algorithm is $O(\max[\mathcal{A}, N \log_2 M]MJ^2)$.

Remarks

1. The fast Hilbert transform algorithm can be used to obtain the Bermudan put option values at varying values of S_0 simultaneously with almost no additional cost. Also, the option delta and gamma can be obtained with essentially no additional computational effort. Specifically, the last step Eq. (4.11) can be slightly modified to compute the option delta

$$\begin{aligned} & \frac{\partial V(Y_{t_0}, \zeta_p, t_0)}{\partial S_0} \\ & \approx - \frac{e^{-r\Delta}}{2\pi S_0} \sum_{j=1}^J w_j \sum_{m=-M}^M (\alpha + imh) e^{-(\alpha + imh)Y_{t_0}} \hat{V}_\alpha(mh, \zeta_j, t_1) \tilde{\Psi}(-\alpha - imh; \zeta_j, \zeta_p) h. \end{aligned}$$

2. In our fast Hilbert transform algorithm for pricing Bermudan options under time-changed Lévy processes, the same Toeplitz matrix can be used from one time step to the next. Only two runs of the fast Fourier transform are required for each time

step, exhibiting exponentially decaying pricing errors. Fang and Oosterlee (2011) propose a Fourier-cosine series expansion approach to price Bermudan options under the Heston model. The discrete approximation in their algorithm is implemented using the Toeplitz and Hankel matrix-vector multiplications. However, the corresponding Toeplitz and Hankel matrices are time-variant matrices. Furthermore, the Fourier-cosine algorithm requires five runs of the fast Fourier transform for each time step.

5 Numerical tests on the Hilbert transform algorithms

In this section, we would like to demonstrate the performance of the fast Hilbert transform algorithms for pricing the dividend-ruin model and Bermudan put options under two choices of time-changed Lévy processes: Heston’s stochastic volatility model and Normal Inverse Gaussian process time-changed by the CIR process.

5.1 Dividend-ruin model

We present sample calculations for finding the firm asset value function in the dividend-ruin model where the firm asset value process follows a time-changed Lévy process. In our first test case, we choose the underlying asset process to follow the Heston model. The following set of parameter values of the Heston model for pricing the dividend-ruin model are used in our sample calculations (see Table 1). The Heston model parameter values are obtained by minimizing the sum of squared pricing errors between the market prices of S&P 500 options and the model-determined prices (Bakshi *et al.*, 1997).

A_0	T	B	L	r	λ	η	\bar{v}	v_0	ρ
10	1	13	7	0.04	1.15	0.39	0.0348	0.0348	-0.64

Table 1: Parameter values of the Heston model for pricing the dividend-ruin model

Recall that $\nu = \frac{2\lambda\bar{v}}{\eta^2} - 1$ and the satisfaction of the Feller condition is equivalent to $\nu \geq 0$ (see Appendix A). For the above model parameters obtained from the market options data, it is seen that $\nu = -0.47 < 0$. Therefore, the CIR process as specified by the model parameters in Table 1 does not satisfy the Feller condition. In this case, the left tail of the activity rate density grows extremely fast in value. Thanks to the transformation from the activity rate domain to the log-activity rate domain, we manage to obtain very accurate numerical results using the fast Hilbert transform algorithm. To demonstrate the impact of the violation of the Feller condition, we also consider another case with λ set to be 2.5 while all other parameters remain unchanged. In this case, the Feller condition is satisfied. For both cases, the numerical results for the firm asset value function obtained from the fast Hilbert transform algorithm with varying number of monitoring instants N are compared with the benchmark results obtained using the Monte Carlo method (see Table 2). Good agreement of the numerical results from the two numerical methods is observed. This confirms high level of accuracy of the fast Hilbert transform algorithm even under the scenario where the Feller condition fails. We also report the CPU times required for the numerical computation using the Hilbert transform algorithm. It takes a longer time to achieve the same level of accuracy when the Feller condition fails. The failure of the Feller condition leads to the phenomenon where the left-side tail of the log-activity rate density function converges slower to zero. Consequently, we have to set the truncation range in the log-activity rate dimension to be wider in order to achieve the same tolerance level in numerical accuracy.

When performing numerical calculations in a wider truncation range, a larger value of J is required for the same level of accuracy. Note that $J = 2^7$ is used when $\lambda = 2.5$ while $J = 2^8$ when $\lambda = 1.15$. With regard to pricing behavior, the firm asset value is seen to decrease as the number of monitoring instants increases. That is consistent with financial intuition that higher frequency of monitoring leads to greater loss in the firm asset value.

λ	J	N	Hilbert Transform	Monte Carlo	RE(%)	Time (sec)
2.5	2^7	60	9.3938	9.3921 (0.0052)	0.02	30.8
		90	9.3668	9.3738 (0.0053)	0.07	38.1
		120	9.3564	9.3662 (0.0054)	0.10	46.1
1.15	2^8	60	9.3417	9.3528 (0.0054)	0.12	156.0
		90	9.3194	9.3363 (0.0054)	0.18	171.5
		120	9.3123	9.3257 (0.0055)	0.14	199.9

Table 2: Comparison of the numerical results for the firm asset value obtained from the fast Hilbert transform algorithm (truncation level parameter: $M = 2^8$ and damping factor: $\alpha = -4$) with the benchmark results obtained using the Monte Carlo method with $\mathcal{M} = 10^5$ simulation paths. The numerical values shown in brackets are the standard errors in the Monte Carlo simulation. RE denotes the relative percentage error using the fast Hilbert transform algorithm. The required computational time to achieve the same level of numerical accuracy is several times more when the Feller condition is not satisfied (corresponding to $\lambda = 1.15$).

Next, we would like to examine the rate of convergence of the fast Hilbert transform algorithm with regard to M (truncation level parameter in the log-asset return dimension). We compute the benchmark price for the fast Hilbert transform algorithm by taking a sufficiently large value of $M = 16,384$ for $N = 120$. As revealed from Figure 1, the numerical results exhibit exponential rate of decay of the pricing error with respect to M , confirming with similar observations in the numerical performance of the fast Hilbert transform algorithm reported in Feng and Linetsky (2008). Figure 2 shows the firm asset value function $V(Z_{t_0}, \gamma_{t_0}, t_0)$ as a function of initial firm asset value A_0 . We also compare the firm asset value function with and without the embedded ruin and dividend barrier features at varying values of initial firm asset value A_0 .

Next, we consider pricing of the firm asset value under the NIG-CIR model, which is a time-changed Lévy process having the Normal Inverse Gaussian process as the base Lévy process and the CIR process as the activity rate process of time change. The characteristic function of the Normal Inverse Gaussian process is given by

$$\phi_t(\xi) = \exp \left(i\mu t \xi - \delta_{NIG} t \left(\sqrt{\alpha_{NIG}^2 - (\beta_{NIG} + i\xi)^2} - \sqrt{\alpha_{NIG}^2 - \beta_{NIG}^2} \right) \right), \quad (5.1a)$$

where μ is determined by the martingale condition to be

$$\mu = \delta_{NIG} \left(\sqrt{\alpha_{NIG}^2 - (\beta_{NIG} + 1)^2} - \sqrt{\alpha_{NIG}^2 - \beta_{NIG}^2} \right). \quad (5.1b)$$

For the NIG process, we have $(\lambda_-, \lambda_+) = (\beta_{NIG} - \alpha_{NIG}, \beta_{NIG} + \alpha_{NIG})$. The parameter values of the NIG-CIR process for pricing the dividend-ruin model used in our sample calculations are listed in Table 3, which are taken from the same set of parameter values obtained in Schoutens and Symens (2002) from their calibration to the *S&P* 500 option prices. For the given set of model parameter values in Table 3, one can check that $\nu = -0.5182 < 0$, signifying the failure of the Feller condition of the CIR process.

A_0	T	r	N	α_{NIG}	β_{NIG}	δ_{NIG}	λ	η	\bar{v}	v_0
10	0.75	0.04	100	18.4815	-4.8412	0.4685	0.5391	1.8772	1.5746	1

Table 3: Parameter values of the NIG-CIR process for pricing the dividend-ruin model.

We resort to the Monte Carlo method to obtain benchmark results for comparison of accuracy. In the Monte Carlo procedure, the key step involves approximating the Lévy process by the compound Poisson process (Schoutens and Symens, 2002). In Table 4, we show the comparison of the numerical results using the fast Hilbert transform method and the Monte Carlo method for varying set of values for the upper barrier and lower barrier.

B	L	Monte Carlo	$M = 2^8$			$M = 2^9$		
			HT	RE(%)	Time (sec)	HT	RE(%)	Time (sec)
12	8	9.0279 (0.0071)	9.0187	0.10	172.6	9.0343	0.07	342.6
12	7	9.6227 (0.0040)	9.6410	0.19	172.8	9.6266	0.04	342.2
13	8	9.1347 (0.0069)	9.1232	0.13	172.6	9.1312	0.04	342.4
13	7	9.7238 (0.0037)	9.7083	0.16	171.9	9.7160	0.08	342.3
14	6	9.9295 (0.0017)	9.9212	0.08	172.7	9.9247	0.05	342.9

Table 4: Comparison of the numerical results for the firm asset value obtained from the fast Hilbert transform algorithm (truncation level parameter: $J = 2^8$ and damping factor: $\alpha = -5$) with the benchmark results obtained using the Monte Carlo method with $\mathcal{M} = 10^5$ simulation paths. The numerical values shown in brackets are the standard errors in the Monte Carlo simulation. HT denotes the numerical results obtained from the fast Hilbert transform algorithm.

Due to computational convenience achieved by adopting the log-activity rate, the proposed Hilbert transform algorithm works well even under the failure of the Feller condition. As shown in Table 4, higher value of M leads to higher level of numerical accuracy at the cost of computational times. Intuitively, when B and L are sufficiently far from $A_0 = 10$, the firm asset value function becomes quite close to the initial firm asset value. This is consistent with the numerical results shown in Table 4, where the firm asset value equals 9.92 (only 0.08 below $A_0 = 10$ in value) when $B = 14$ and $L = 6$.

5.2 Bermudan options

We now consider pricing Bermudan put options under time-changed Lévy processes. Firstly, we assume the underlying asset process to follow the Heston model. The parameter values in the Bermudan put option are shown in Table 5, which are taken from the most commonly used set of parameters for pricing American options under the Heston model in the literature (Fang and Oosterlee, 2011).

K	T	r	λ	η	\bar{v}	v_0	ρ
10	0.25	0.1	5	0.9	0.16	0.0625	0.1

Table 5: Parameter values of the Heston model for pricing the Bermudan put option.

The numerical results for the Bermudan put option values using the fast Hilbert transform algorithm for varying number of monitoring time instants N and initial asset price S_0 are

presented in Table 6, while those obtained using the Fourier cosine method in Fang and Oosterlee (2011) are also listed in brackets for comparison. The convergence of the Bermudan put option values to the American option values (corresponding to $N \rightarrow \infty$) is clearly observed. The CPU times required in the computation are reported in the last column.

$N \setminus S_0$	8	9	10	11	12	Time (sec)
10	1.98200 (1.98200)	1.10287 (1.10283)	0.51722 (0.51718)	0.21239 (0.21237)	0.08153 (0.08153)	6.56 (6.91)
20	1.99047 (1.99046)	1.10531 (1.10523)	0.51872 (0.51863)	0.21307 (0.21301)	0.081791 (0.08177)	7.17 (7.49)
40	1.99488 (1.99486)	1.10671 (1.10655)	0.51967 (0.51948)	0.21355 (0.21342)	0.08199 (0.08192)	8.42 (8.89)
80	1.99719 (1.99717)	1.10760 (1.10733)	0.52007 (0.52006)	0.21367 (0.21373)	0.08200 (0.08204)	11.76 (14.05)
American put value	2.000000	1.107621	0.520030	0.213677	0.082044	NA

Table 6: Comparison of the numerical results for Bermudan put option values obtained from the fast Hilbert transform algorithm (truncation level parameters: $M = 2^6$, $J = 2^7$ and damping factor: $\alpha = 5$) with those obtained using the Fourier cosine method (shown in brackets).

Table 6 reveals good numerical performance of the fast Hilbert transform method when compared with the performance of the Fourier cosine method (known to be a reliable and accurate method to price Bermudan options under the Heston model). These observations confirm high level of accuracy and efficiency of the fast Hilbert transform method. Another advantage of our method is that it is applicable to the general class of time-changed Lévy processes, not necessarily limited to the Heston model. Note that the numerical performance of the fast Hilbert transform algorithm depends on the tail behavior of the conditional moment generating function $\Psi_\Delta(-\alpha - i\beta; \zeta_j, \zeta_p)$. For a smaller value of Δ , it decays slower, so larger value of M may be required to achieve a given level of tolerance of truncation error. Therefore, pricing Bermudan options with higher monitoring frequency is computationally more demanding.

We also explore the dependence of the critical asset prices on time to maturity for varying values of fixed activity rate v . Figure 3 shows that the critical asset prices decrease when the time to maturity lengthens and higher activity rate leads to lower critical asset price. Next, we investigate the dependence of the Bermudan put option value and option delta on the initial asset price S_0 for varying values of the initial activity rate v_0 . Figure 4 shows that the Bermudan put option value is an increasing function of the initial activity rate v_0 . Figure 5 reveals that the put option delta is an increasing function of S_0 and the put option delta values shows a more moderate rate of change in values at a higher level of v_0 .

In the next set of sample calculations, we adopt the same set of parameter values of the Heston model from Table 1. We set $K = 100$ and $T = 0.25$ for the Bermudan put option. Recall that the computational effort in the preparation step with non-equidistant quadrature rules is dominated by the computation of the matrices $\tilde{\Psi}(\zeta_p)$, $p = 1, 2, \dots, J$, which involve numerical valuation of the modified Bessel functions. The entries under the column “Init” in Tables 7 and 8 show the CPU times in the preparation step, which are shown to dominate the total running CPU time. We use “Loop” to denote the running CPU time for the looping step in the fast Hilbert transform algorithm and Fourier cosine method. The sum of “Init” and “Loop” gives the total CPU time. Table 7 lists the results of the numerical tests that were performed to examine accuracy and efficiency of the fast Hilbert transform algorithm, while those obtained by the Fourier cosine method are listed in brackets.

S_0	90	100	110	total	Init	Loop
$N = 20$	9.97861 (9.97837)	3.20410 (3.20474)	0.92691 (0.92811)	62.2 (68.9)	54.8 (59.3)	7.4 (10.7)
$N = 40$	9.99291 (9.99165)	3.20719 (3.20733)	0.92772 (0.92811)	73.1 (81.9)	55.7 (59.3)	17.4 (22.6)
$N = 60$	9.99799 (9.99578)	3.20856 (3.20792)	0.92808 (0.92804)	83.0 (93.2)	58.1 (59.4)	24.9 (33.8)

Table 7: Comparison of the numerical results for the Bermudan put option values obtained from the fast Hilbert transform algorithm (truncation level parameters: $M = 2^7$, $J = 2^8$ and damping factor: $\alpha = 5$) with those obtained using the Fourier cosine method (shown in brackets).

Lastly, we also consider pricing Bermudan put options under the general time-changed Lévy processes. Likewise, we take the underlying asset to follow the NIG-CIR process in our sample calculations using the same set of parameter values from Table 3, except that $T = 0.25$. Table 8 lists the numerical results for Bermudan put option values for varying values of initial asset price S_0 . Our numerical experiments show that relatively large values of the truncation level parameters ($M = 2^9$ and $J = 2^8$) are required in order to achieve accuracy less than 0.2% in relative percentage error. Since reference values for comparison are not available in the literature, the numerical results provided in Table 8 may serve as benchmark values for comparison with numerical results obtained from future pricing methods.

S_0	9	10	11	total	Init.	Loop
$N = 10$	0.97768	0.23234	0.05212	234.2	217.9	16.3
$N = 20$	0.98858	0.23363	0.05239	250.9	218.3	32.6
$N = 30$	0.99233	0.23406	0.05248	281.6	218.9	62.7

Table 8: Numerical results for Bermudan put option values obtained from the fast Hilbert transform algorithm (truncation level parameters: $M = 2^9$, $J = 2^8$ and damping factor: $\alpha = 5$) under the NIG-CIR model.

6 Conclusion

We develop and apply the effective fast Hilbert transform algorithms for pricing dividend-ruin model with default and dividend barrier features and Bermudan options under time-changed Lévy processes. The renowned Heston model as an affine stochastic volatility model is nested within the class of time-changed Lévy processes. It is a non-trivial generalization of the fast Hilbert transform method that has been developed earlier for option pricing under one-dimensional Lévy processes. Our pricing algorithms under time-changed Lévy processes are derived by applying the fast Hilbert transform method in the log-asset return dimension and a quadrature rule in the log-activity rate dimension. The option delta and gamma can also be obtained with essentially no additional computational effort.

In view of the near-singular behavior of the probability density of the activity rate, a transformation from the activity rate domain to the log-activity rate domain has been chosen in the construction of the fast Hilbert transform algorithms. The finite time dividend-ruin

model resembles a path dependent option model with both the lookback and barrier feature, so it is more complex to be priced compared to the barrier options. Besides incorporating the knock-out barrier, we also extend the fast Hilbert transform algorithm for pricing discrete options with reflecting style barrier under the Lévy setting to time-changed Lévy processes. In fact, we provide a framework of using the fast Hilbert transform method to price any options with absorbing or reflecting barrier feature and defaultable bonds under time-changed Lévy processes. We also show how to combine the fast Hilbert transform method and quadrature rule to price Bermudan options under the framework of time-changed Lévy processes. We prove the existence of unique critical asset price for determining the optimal exercise decision in the Bermudan put option under time-changed Lévy processes. We compare the numerical performance of the fast Hilbert transform algorithm with the Fourier cosine method. The fast Hilbert transform method is seen to be highly accurate and more efficient compared to other existing algorithms.

The computational cost of the method is approximately $O(\max[\mathcal{A}, N \log_2 M] M J^2)$, where N is the number of monitoring instants, and M and J are the truncation level parameters in the log-asset return dimension and log-activity rate dimension, respectively. High efficiency, accuracy, reliability and robustness of the fast Hilbert algorithms are demonstrated through various numerical tests in pricing dividend-ruin models and Bermudan options under the Heston model and NIG-CIR model. High level of numerical accuracy is observed even under the scenario where the Feller condition in the CIR process of the activity rate is not satisfied.

REFERENCES

- Aitsahlia, F., and Lai, T.L. (1998). Random walk duality and the valuation of discrete lookback options. *Applied Mathematical Finance*, **5**, 227-240.
- Andersen, L. (2008). Simple and efficient simulation of the Heston stochastic volatility model. *Journal of Computational Finance*, **11**, 1-42.
- Andreasen, J. (1998). The pricing of discretely sampled Asian and lookback options: a change of numeraire approach. *Journal of Computational Finance*, **2**, 5-30.
- Atkinson, C., and Fusai, G. (2007). Discrete extreme of Brownian motion and pricing of exotic options. *Journal of Computational Finance*, **10(3)**, 1-43.
- Bakshi, G., Cao, C., and Chen, Z. (1997). Empirical performance of alternative option pricing models. *The Journal of Finance*, **52(5)**, 2003-2049.
- Broadie, M., and Glasserman, P, and Kou, S. (1997). A continuity correction for discrete barrier options. *Mathematical Finance*, **7(4)**, 325-349.
- Broadie, M., and Glasserman, P, and Kou, S. (1999). Connecting discrete and continuous path-dependent options. *Finance and Stochastics*, **3**, 55-82.
- Broadie, M., and Kaya, Ö. (2006). Exact simulation of stochastic volatility and other affine jump diffusion processes. *Operations Research*, **54(2)**, 217-231.
- Broadie, M., and Yamamoto, Y. (2005). A double-exponential fast Gauss transform algorithm for pricing discrete path-dependent options. *Operations Research*, **53(5)**, 764-779.
- Carr, P., and Wu, L.R. (2004). Time-changed Lévy processes and option pricing. *Journal of Financial Economics*, **71**, 113-141.
- Carr, P., Geman, H., Madan, D., and Yor, M. (2003). Stochastic volatility for Lévy processes. *Mathematical Finance*, **13**, 345-382.
- Cox, J.C., Ingersoll, J.E., and Ross, S.A. (1985). A theory of the term structure of interest rates. *Econometrica*, **53(2)**, 385-407.
- Dia, E.H.A., and Lamberton, D. (2011). Continuity correction for barrier options in jump diffusion models. *SIAM Journal on Financial Mathematics*, **2(1)**, 866-900.
- Duan, J.C., Dudley, E., Gauthier, G., and Simonato, J.G. (2003). Pricing discretely monitored barrier options by a Markov chain. *Journal of Derivatives*, **10(4)**, 9-31.
- Fang, F., and Oosterlee, C.W. (2011). A Fourier-based valuation method for Bermudan and barrier options under Heston's Model. *SIAM Journal on Financial Mathematics*, **2(1)**, 439-463.
- Feng, L., and Linetsky, V. (2008). Pricing discretely monitored barrier options and defaultable bonds in Lévy process models: a fast Hilbert transform approach. *Mathematical Finance*, **18(3)**, 337-384.
- Feng, L., and Linetsky, V. (2009). Computing exponential moments of the discrete maximum of a Levy process and lookback options. *Finance and Stochastics*, **13(4)**, 501-529.
- Feng, L., and Lin, X. (2013). Pricing Bermudan options in Lévy process models. To appear in *SIAM Journal on Financial Mathematics*.
- Fusai, G., Abrahams, I.D, and Sgarra, C. (2006). An exact analytical solution for discrete barrier options. *Finance and Stochastics*, **10**, 1-26.
- Fusai, G, and Recchioni, M.C. (2007). Analysis of quadrature methods for pricing discrete barrier options. *Journal of Economic and Dynamic Control*, **31**, 826-860.

- Heynen, R.C., and Kat, H.M. (1995). Lookback options with discrete and partial monitoring of the underlying price. *Applied Mathematical Finance*, **2**, 273-284.
- Ito, K., and Toivanen, J. (2009). Lagrange multiplier approach with optimized finite difference stencils for pricing American options under stochastic volatility. *SIAM Journal on Scientific Computing*, **31**, 2646-2664.
- Jackson, K.R., Jaimungal, S., and Surkov, V. (2008). Fourier space time-stepping for option pricing with Lévy models. *Journal of Computational Finance*, **12(2)**, 1-29.
- Kim, Y. S., Fabozzi, F. J., Lin, Z., and Rachev, S. T. (2012). Option pricing and hedging under a stochastic volatility Lévy process model. *Review of Derivatives Research*, **15(1)**, 81-97..
- King, F.W. (2009). *Hilbert Transforms*. Cambridge University Press, Cambridge, United Kingdom.
- Kou, S.G. (2008). Discrete barrier and lookback options. *Handbooks in Operations Research and Management Science*, **15**, 343-373.
- Küchler, U., and Sorensen, M. (1997). *Exponential families of stochastic processes*. Springer Series in Statistics, Springer, New York.
- Kwok, Y.K., Leung, K.S., and Wong, H.Y. (2012). Efficient options pricing using the fast Fourier transform. *Handbook of Computational Finance*, edited by Duan, J.C., Hardle, W.K., and Gentle, J.E., chapter 21, 579-604, Springer, Berlin, Germany.
- Leung, K.S., Kwok, Y.K., and Leung, S.Y. (2008). Finite time dividend-ruin models. *Insurance: Mathematics and Economics*, **42**, 154-162.
- Lindsay, A.E., and Brecher, D.R. (2012). Simulation of the CEV process and the local martingale property. *Mathematics and Computers in Simulation*, **82(5)**, 868-878.
- Lord, R., Fang, F., Bervoets, F., and Oosterlee, C.W. (2008). A fast and accurate FFT-based method for pricing early-exercise options under Lévy processes. *SIAM Journal on Scientific Computing*, **30**, 1678-1705.
- Petrella, G., and Kou, S. (2004). Numerical pricing of discrete barrier and lookback options via Laplace transform. *Journal of Computational Finance*, **8(1)**, 1-37.
- Sato, K. I. (1999). *Lévy processes and infinitely divisible distributions*. Cambridge University Press.
- Schoutens, W., and Symens, S. (2003). The pricing of exotic options by Monte-Carlo simulations in a Lévy market with stochastic volatility. *International Journal of Theoretical and Applied Finance*, **6**, 839-864.
- Tse, W.M., Li, L.K., and Ng, K.W. (2001). Pricing discrete barrier and hindsight options with the tridiagonal probability algorithm. *Management Science*, **47(3)**, 383-393.
- Wu, L.R. (2008). Modeling financial security returns using Lévy process. *Handbooks in Operations Research and Management Science*, **15**, 117-162.
- Zhylyevskyy, O. (2010). A fast Fourier transform technique for pricing American options under stochastic volatility. *Review of Derivatives Research*, **13**, 1-24.
- Zvan, R., Vetzal, K.R., and Forsyth, P.A. (2000). PDE methods for pricing barrier options. *Journal of Economic Dynamic and Control*, **24**, 1563-1590.

Appendix A. Properties of the CIR process

Consider the CIR process v_t as governed by Eq. (2.5), the distribution of v_t given v_s , $t > s$, is a noncentral chi-squared distribution (up to a scale factor). In terms of the following parameters

$$\nu = \frac{2\lambda\bar{v}}{\eta^2} - 1 \quad \text{and} \quad \zeta = \frac{2\lambda}{[1 - e^{-\lambda(t-s)}]\eta^2},$$

the transition law of v_t can be expressed as (Cox *et al.*, 1985)

$$v_t = \frac{1}{2\zeta} \chi_{2(\nu+1)}^2 [2\zeta e^{-\lambda(t-s)} v_s], \quad t > s, \quad (\text{A.1})$$

where $\chi_{2(\nu+1)}^2(m)$ denotes the noncentral chi-squared random variable with $2(\nu + 1)$ degrees of freedom and noncentrality parameter m . The probability density function of v_t given v_s , $s < t$, can be written as

$$p(v_t|v_s) = \zeta e^{-\zeta[v_s e^{-\lambda(t-s)} + v_t]} \left[\frac{e^{\lambda(t-s)} v_t}{v_s} \right]^{\frac{\nu}{2}} I_\nu \left(2\zeta e^{-\frac{1}{2}\lambda(t-s)} \sqrt{v_s v_t} \right), \quad s < t,$$

where $I_\nu(\cdot)$ is the modified Bessel function of the first kind with order ν . The Feller condition is equivalent to “ $\nu \geq 0$ ”.

We would like to explain why the transformation from the variance domain to the log-variance domain leads to computational convenience that resolves the singular behavior when the CIR model parameters obtained from calibration of real market data fail to satisfy the Feller condition. Let $\gamma_t = \ln v_t$, the conditional density of the log-activity rate process γ_t can be obtained as follows:

$$p_\gamma(\gamma_t|\gamma_s) = \zeta e^{-\zeta[e^{\gamma_s} e^{-\lambda(t-s)} + e^{\gamma_t}]} \left[e^{\gamma_t - \gamma_s} e^{\lambda(t-s)} \right]^{\frac{\nu}{2}} e^{\gamma_t} I_\nu \left(2\zeta e^{-\frac{1}{2}\lambda(t-s)} \sqrt{e^{\gamma_t} e^{\gamma_s}} \right). \quad (\text{A.2})$$

The appearance of the term e^{γ_t} compensates the $(\cdot)^{\frac{\nu}{2}}$ term, so the conditional density of log-activity rate converges to zero as $\gamma_t \rightarrow -\infty$. Compared to the conditional density of activity rate, the new form of conditional density demonstrates two main advantages. Firstly, the left tail of the conditional density of log-activity rate decays to zero rapidly instead of increasing significantly, though the decay rate may decrease when ν approaches -1 . Secondly, the conditional densities of the log-activity rate processes for different parameter values are more symmetric than those of the activity rate processes.

Broadie and Kaya (2006) use the Fourier inversion technique to invert the characteristic function of the time-integrated variance $\int_s^t v_u \, du$ to generate a sample for the integral. The closed form expression for the characteristic function conditional on v_t and v_s is given by (Broadie and Kaya, 2006)

$$\begin{aligned} \Phi(\xi; \gamma_t, \gamma_s) &= E \left[e^{i\xi \int_s^t v_u \, du} \middle| \gamma_t, \gamma_s \right] \\ &= \frac{I_\nu \left(\sqrt{e^{\gamma_t} e^{\gamma_s}} \frac{4\tilde{\gamma}(\xi) e^{-\frac{1}{2}\tilde{\gamma}(\xi)(t-s)}}{\eta^2 [1 - e^{-\tilde{\gamma}(\xi)(t-s)}]} \right)}{I_\nu \left(\sqrt{e^{\gamma_t} e^{\gamma_s}} \frac{4\lambda e^{-\frac{1}{2}\lambda(t-s)}}{\eta^2 [1 - e^{-\lambda(t-s)}]} \right)} \frac{\tilde{\gamma}(\xi) e^{-\frac{1}{2}[\tilde{\gamma}(\xi) - \lambda](t-s)} [1 - e^{-\lambda(t-s)}]}{\lambda [1 - e^{-\tilde{\gamma}(\xi)(t-s)}]} \\ &\quad \exp \left(\frac{e^{\gamma_s} + e^{\gamma_t}}{\eta^2} \left\{ \frac{\lambda [1 + e^{-\lambda(t-s)}]}{1 - e^{-\lambda(t-s)}} - \frac{\tilde{\gamma}(\xi) [1 + e^{-\tilde{\gamma}(\xi)(t-s)}]}{1 - e^{-\tilde{\gamma}(\xi)(t-s)}} \right\} \right), \end{aligned} \quad (\text{A.3})$$

where $\tilde{\gamma}(\xi) = \sqrt{\lambda^2 - 2i\eta^2\xi}$.

Appendix B. Proof of Proposition 1

We denote $Y_t = \ln \frac{S_t}{K} = rt + X_{T_t}$, and write the joint conditional probability density of the difference of the log-asset return and log-activity rate as $p_k(\Delta_k Y, \gamma_{t_{k+1}} | Y_{t_k}, \gamma_{t_k})$, where $\Delta_k Y = Y_{t_{k+1}} - Y_{t_k}$. Let $\tilde{V}(S_{t_k}, \gamma_{t_k}, t_k)$ and $\tilde{C}(S_{t_k}, \gamma_{t_k}, t_k)$ denote the Bermudan put option value and continuation value at time t_k , respectively. For $k = N - 1, N - 2, \dots, 0$, we have

$$\tilde{C}(S_{t_k}, \gamma_{t_k}, t_k) = e^{-r\Delta} E_{t_k} [\tilde{V}(S_{t_{k+1}}, \gamma_{t_{k+1}}, t_{k+1})].$$

Following a similar approach as in Feng and Lin (2013), we establish the proof of the proposition by mathematical induction. For $k = N - 1$, we consider the derivative of $\tilde{V}(S_{t_{N-1}}, \gamma_{t_{N-1}}, t_{N-1})$ with respect to $S_{t_{N-1}}$ as follows

$$\begin{aligned} & \frac{d}{dS_{t_{N-1}}} \tilde{C}(S_{t_{N-1}}, \gamma_{t_{N-1}}, t_{N-1}) \\ &= \frac{d}{dS_{t_{N-1}}} \int_{-\infty}^{\ln \frac{K}{S_{t_{N-1}}}} e^{-r\Delta} (K - S_{t_{N-1}} e^{\Delta_{N-1} Y}) p_{N-1}(\Delta_{N-1} Y | Y_{t_{N-1}}, \gamma_{t_{N-1}}) d\Delta_{N-1} Y \\ &= -e^{-r\Delta} \frac{K - S_{t_{N-1}} e^{\ln \frac{K}{S_{t_{N-1}}}}}{S_{t_{N-1}}} p_{N-1}\left(\ln \frac{K}{S_{t_{N-1}}} | Y_{t_{N-1}}, \gamma_{t_{N-1}}\right) \\ &\quad - e^{-r\Delta} \int_{-\infty}^{\ln \frac{K}{S_{t_{N-1}}}} e^{\Delta_{N-1} Y} p_{N-1}(\Delta_{N-1} Y | Y_{t_{N-1}}, \gamma_{t_{N-1}}) d\Delta_{N-1} Y \\ &> -e^{-r\Delta} \int_{-\infty}^{\infty} e^{\Delta_{N-1} Y} p_{N-1}(\Delta_{N-1} Y | Y_{t_{N-1}}, \gamma_{t_{N-1}}) d\Delta_{N-1} Y \\ &= -e^{-r\Delta} E_{t_{N-1}} [e^{\Delta_{N-1} Y}] = -E_{t_{N-1}} [e^{X_{T_N} - X_{T_{N-1}}}] = -1. \end{aligned}$$

The last equality holds by virtue of the martingale property of X_{T_t} . Since $\tilde{C}(S_{t_{N-1}}, \gamma_{t_{N-1}}, t_{N-1}) > 0$ for any $S_{t_{N-1}} > 0$, and

$$\lim_{S_{t_{N-1}} \rightarrow 0^+} \tilde{C}(S_{t_{N-1}}, \gamma_{t_{N-1}}, t_{N-1}) = Ke^{-r\Delta},$$

there exists unique critical asset price $S_{N-1}^*(\gamma_{t_{N-1}})$ satisfying $0 < S_{N-1}^*(\gamma_{t_{N-1}}) < K$, such that

$$\tilde{G}(S_{t_{N-1}}) = \tilde{C}(S_{t_{N-1}}, \gamma_{t_{N-1}}, t_{N-1}).$$

Once $S_{N-1}^*(\gamma_{t_{N-1}})$ is determined, the Bermudan put option value at t_{N-1} is given by

$$\begin{aligned} \tilde{V}(S_{t_{N-1}}, \gamma_{t_{N-1}}, t_{N-1}) &= e^{-r\Delta} E_{t_{N-1}} [\tilde{V}(S_{t_N}, \gamma_{t_N}, t_N)] \mathbf{1}_{(S_{N-1}^*(\gamma_{t_{N-1}}), \infty)} \\ &\quad + \tilde{G}(S_{t_{N-1}}) \mathbf{1}_{(0, S_{N-1}^*(\gamma_{t_{N-1}}))}. \end{aligned}$$

Suppose the formula holds for $k + 1$, where $2 \leq k + 1 \leq N - 1$, we would like to show that it is also true for k . Similarly, we consider the derivative of $\tilde{V}(S_{t_k}, \gamma_{t_k}, t_k)$ with respect

to S_{t_k} as follows

$$\begin{aligned}
& \frac{d}{dS_{t_k}} \tilde{C}(S_{t_k}, \gamma_{t_k}, t_k) \\
&= \frac{d}{dS_{t_k}} \int_{-\infty}^{\ln \frac{S_{k+1}^*(\gamma_{t_{k+1}})}{S_{t_k}}} \int_{-\infty}^{\infty} e^{-r\Delta} (K - S_{t_k} e^{\Delta_k Y}) p_k(\Delta_k Y, \gamma_{t_{k+1}} | Y_{t_k}, \gamma_{t_k}) d\gamma_{t_{k+1}} d\Delta_k Y \\
&\quad + \frac{d}{dS_{t_k}} \int_{\ln \frac{S_{k+1}^*(\gamma_{t_{k+1}})}{S_{t_k}}}^{\infty} \int_{-\infty}^{\infty} e^{-r\Delta} \tilde{C}(S_{t_k} e^{\Delta_k Y}, \gamma_{t_{k+1}}, t_{k+1}) p_k(\Delta_k Y, \gamma_{t_{k+1}} | Y_{t_k}, \gamma_{t_k}) d\gamma_{t_{k+1}} d\Delta_k Y \\
&= -e^{-r\Delta} \int_{-\infty}^{\infty} \frac{K - S_{k+1}^*(\gamma_{t_{k+1}})}{S_{t_k}} p_k\left(\ln \frac{S_{k+1}^*(\gamma_{t_{k+1}})}{S_{t_k}}, \gamma_{t_{k+1}} | Y_{t_k}, \gamma_{t_k}\right) d\gamma_{t_{k+1}} \\
&\quad - e^{-r\Delta} \int_{-\infty}^{\ln \frac{S_{k+1}^*(\gamma_{t_{k+1}})}{S_{t_k}}} \int_{-\infty}^{\infty} e^{\Delta_k Y} p_k(\Delta_k Y, \gamma_{t_{k+1}} | Y_{t_k}, \gamma_{t_k}) d\gamma_{t_{k+1}} d\Delta_k Y \\
&\quad + e^{-r\Delta} \int_{-\infty}^{\infty} \frac{\tilde{C}(S_{k+1}^*(\gamma_{t_{k+1}}), \gamma_{t_{k+1}}, t_{k+1})}{S_{t_k}} p_k\left(\ln \frac{S_{k+1}^*(\gamma_{t_{k+1}})}{S_{t_k}}, \gamma_{t_{k+1}} | Y_{t_k}, \gamma_{t_k}\right) d\gamma_{t_{k+1}} \\
&\quad + e^{-r\Delta} \int_{\ln \frac{S_{k+1}^*(\gamma_{t_{k+1}})}{S_{t_k}}}^{\infty} \int_{-\infty}^{\infty} \frac{d\tilde{C}(S_{t_k} e^{\Delta_k Y}, \gamma_{t_{k+1}}, t_{k+1})}{dS_{t_k}} e^{\Delta_k Y} p_k(\Delta_k Y, \gamma_{t_{k+1}} | Y_{t_k}, \gamma_{t_k}) d\gamma_{t_{k+1}} d\Delta_k Y \\
&\geq -e^{-r\Delta} \int_{-\infty}^{\ln \frac{S_{k+1}^*(\gamma_{t_{k+1}})}{S_{t_k}}} \int_{-\infty}^{\infty} e^{\Delta_k Y} p_k(\Delta_k Y, \gamma_{t_{k+1}} | Y_{t_k}, \gamma_{t_k}) d\gamma_{t_{k+1}} d\Delta_k Y \\
&\quad - e^{-r\Delta} \int_{\ln \frac{S_{k+1}^*(\gamma_{t_{k+1}})}{S_{t_k}}}^{\infty} \int_{-\infty}^{\infty} e^{\Delta_k Y} p_k(\Delta_k Y, \gamma_{t_{k+1}} | Y_{t_k}, \gamma_{t_k}) d\gamma_{t_{k+1}} d\Delta_k Y \\
&= -e^{-r\Delta} E_{t_k} [e^{\Delta_k Y}] = -E_{t_k} [e^{X_{T_{k+1}}} - X_{T_k}] = -1.
\end{aligned}$$

In the above deviation, we have used the relation:

$$K - S_{k+1}^*(\gamma_{t_{k+1}}) = \tilde{C}(S_{k+1}^*(\gamma_{t_{k+1}}), \gamma_{t_{k+1}}, t_{k+1}).$$

Similarly, since $\tilde{C}(S_{t_k}, \gamma_{t_k}, t_k) > 0$ for any $S_{t_k} > 0$, and $\lim_{S_{t_k} \rightarrow 0^+} \tilde{C}(S_{t_k}, \gamma_{t_k}, t_k) = K e^{-r\Delta}$, there exists a unique critical asset price $S_k^*(\gamma_{t_k})$ satisfying $0 < S_k^*(\gamma_{t_k}) < K$ that solves $\tilde{C}(S_{t_k}, \gamma_{t_k}, t_k) = \tilde{G}(S_{t_k})$, so Eq. (4.1) holds. The proof is completed by the mathematical induction argument.

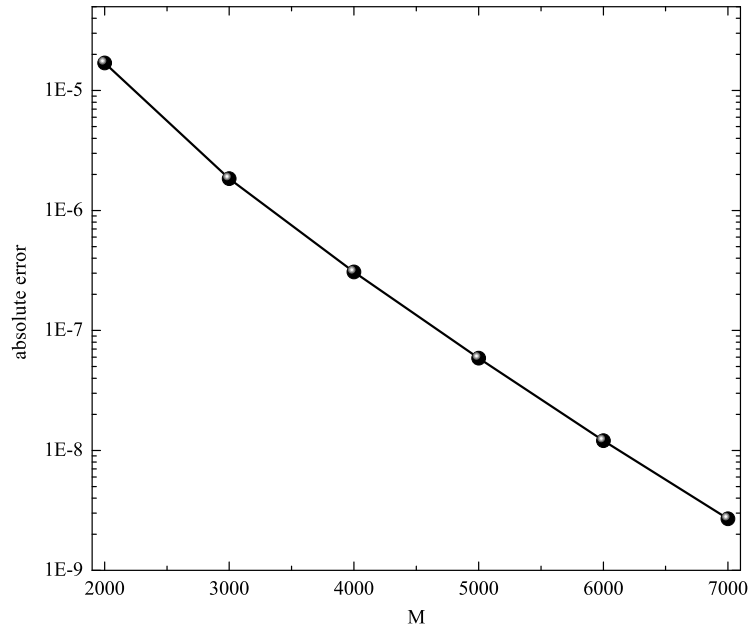


Figure 1: Plot of the absolute errors in the numerical calculations of the firm asset value function using the fast Hilbert transform algorithm against M (truncation level parameter in the log-asset return dimension). The exponential rate of decay of the pricing errors with respect to M is revealed.

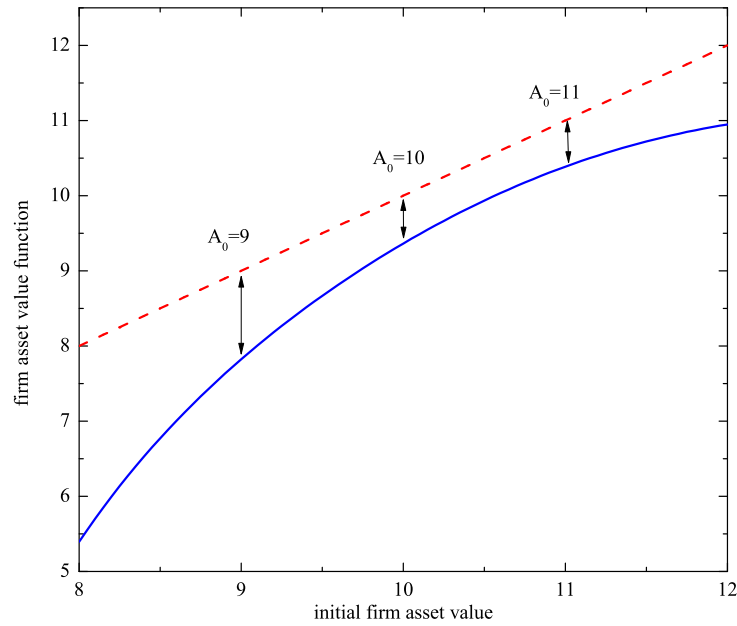


Figure 2: Plot of the firm asset value function $V(Z_{t_0}, \gamma_{t_0}, t_0)$ against initial firm asset value A_0 under the Heston model. The dotted line shows the firm asset value without the embedded ruin and dividend barrier features. The length of the arrow at a specified value of A_0 indicates the loss in the firm asset value function due to the ruin and dividend barrier features.

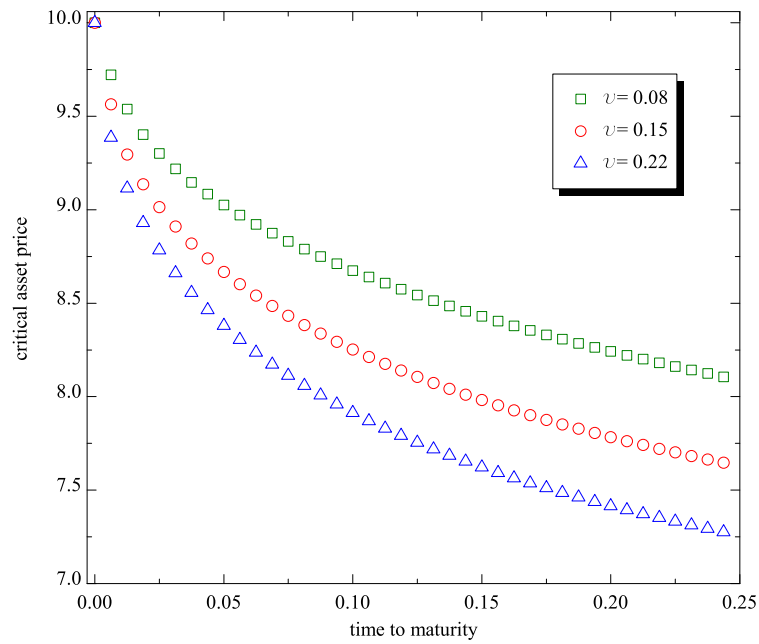


Figure 3: Plots of the critical asset prices against time to maturity of the Bermudan put option under the Heston model for varying values of fixed activity rate v . We observe lower critical asset prices at higher level of v . The impact of v on the critical asset prices can be quite significant for long-lived Bermudan put options.

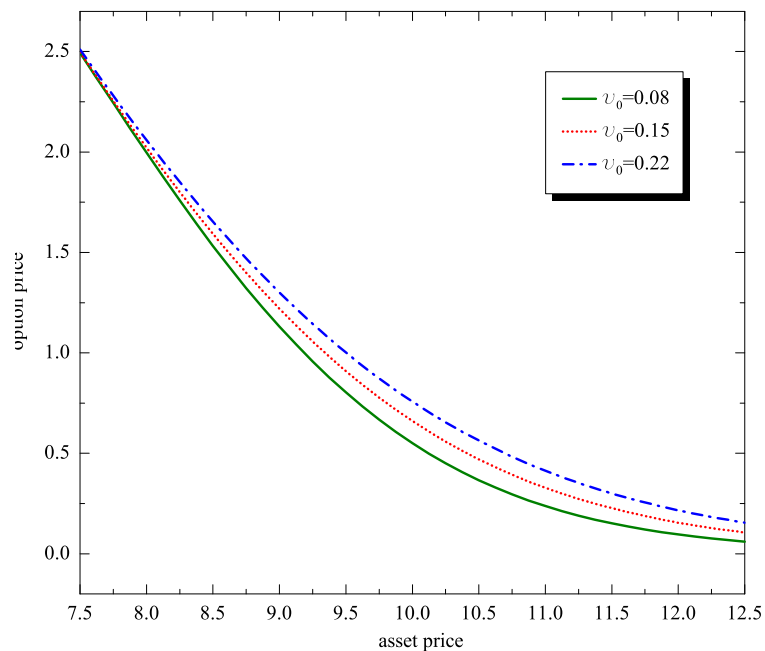


Figure 4: Plots of the Bermudan put option values against initial asset price S_0 under the Heston model for varying values of the initial activity rate v_0 . The Bermudan put option price is seen to be an increasing function of v_0 .

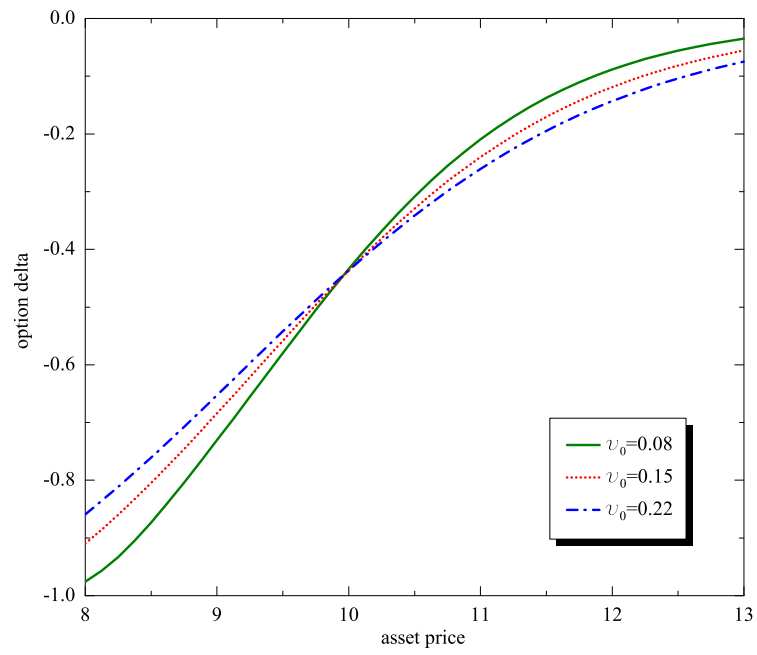


Figure 5: Plots of the Bermudan put option delta against initial asset price S_0 under the Heston model for varying values of the initial activity rate ν_0 .